J. Fluid Mech. (1996), *vol.* 317, *pp.* 241–273

Integral flow properties of the swash zone and averaging

By M. BROCCHINI AND D. H. PEREGRINE †
School of Mathematics, University of Bristol, Bristol, BS8 1TW, UK

(Received 29 July 1995 and in revised form 13 February 1996)

The swash zone is that part of a beach over which the instantaneous shoreline moves back and forth as waves meet the shore. This zone is discussed using the nonlinear shallow water equations which are appropriate for gently sloping beaches. A weakly three-dimensional extension of the two-dimensional solution by Carrier & Greenspan (1958) of the shallow water equations for a wave reflecting on an inclined plane beach is developed and used to illustrate the ideas. Thereafter attention is given to integrated and averaged quantities. The mean shoreline might be defined in several ways, but for modelling purposes we find the lower boundary of the swash zone to be more useful. A set of equations obtained by integrating across the swash zone is investigated as a model for use as an alternative boundary condition for wave-resolving studies. Comparison with sample numerical computations illustrates that they are effective in modelling the dynamics of the swash zone and that a reasonable representation of swash zone flows may be obtained from the integrated variables. The longshore flow of water in the swash zone is in many ways similar to the Stokes' drift of propagating water waves. Further averaging is made over short waves to obtain results suitable as boundary conditions for longer period motions including the effect of incident short waves. In order to clearly present the work a few simplifications are made. The main result is that in addition to the kinematic type of boundary condition that occurs on a simple, e.g. rigid, boundary two further conditions are found in order that both the changing position of the swash zone boundary and the longshore flow in the swash zone may be determined. Models of the short waves both outside and inside the swash zone are needed to complete a full wave-averaged model; only brief indication is given of such modelling.

1. Introduction

The swash zone, i.e. the area of the beach where the waves move the instantaneous shoreline back and forth, is an important, yet little studied, part of the coast. Most applications involving waves in the coastal zone use averaging over many waves, and difficulties associated with averaging hydrodynamic properties in the swash zone are becoming a matter of concern. Many of the available models for the dynamics of waves on shallow water are based on equations for depth-integrated and wave-averaged variables (Mei 1983). Often these models are used to investigate flow properties up to the shoreline e.g. analysis of longshore currents (Van Dongeren *et al.* 1994) and their stability (Dodd 1994). In this context, the boundary conditions

† The author to whom communications should be addressed.

associated with the shoreline need to be properly defined. This involves averaging flow properties where a free moving boundary meets a rigid boundary.

The flow properties in the swash zone are of importance for coastal erosion and accretion, for groundwater flow and flood protection. Also swash motion is of particular relevance because the sediment processes in this zone provide the important boundary condition for the beach evolution. According to some recent studies, longshore sediment transport is closely related to the hydrodynamic motion at the two boundaries of the surf zone i.e. at the breaking point and inside the swash zone. Sediment transport in the swash zone may be considered as a stirring of the sediments by energetic swash and a net transport due to mean longshore currents (Thornton & Abdelrahman 1991). Analysis of the swash zone dynamics is linked, and often confused, with the analysis of the run-up. Predicting the maximal excursion of water on a beach, given the frequency and amplitude of the incident wave train at some distance from the shore, is just one of the goals for research in the field of coastal engineering.

A different perspective is developing for which a more complete analysis of the swash zone motion involves understanding of all aspects of water flow motion in this region where the waterline oscillates, the run-up being just one consequence of those motions. In particular, correct estimates of mass and momentum fluxes inside the swash zone are relevant to the longshore sediment transport. These fluxes are needed as the sum of contributions coming from the motion of waves whose period may range from typical periods of short gravity waves (a few seconds), to much larger periods associated with low-frequency waves (a few minutes) or even with tidal fluctuations (a few hours). A clear concept of mean flow is essential in analysing the effect of all these contributions.

There are strong similarities between the swash zone and the zone between the horizontal planes of the crests and troughs of water waves. For progressing waves the average horizontal flow in that zone is markedly different from the average flow below, and gives the entire contribution to the Stokes' drift mass flow when the waves are appropriately defined and analysed from an Eulerian viewpoint. For a thorough investigation of mass and momentum transfer at the free surface between short- and large-time-scale motions see Hasselmann (1971). One of the main findings is that the above mass transport is relevant to analysis of the interactions between the wave fluctuating field and a mean flow. It is essential to include the divergence of the mass transport term in the kinematic boundary condition for the mean flow (Hasselmann 1971). Similar boundary conditions for the mean flow motion need to be determined at the mean shoreline. In this case a corresponding contribution due to a mean longshore drift velocity needs to be considered.

Here we focus attention on some problems related to the definition of run-up, set-up, the mean shoreline and the averaging of flow properties when a moving boundary (the free surface) meets a fixed boundary (the beach). This study takes the nonlinear shallow water equations to be a suitable model for the swash zone and the nearby region on a beach of gentle slope. A number of studies, e.g. Packwood (1980), Kobayashi, Otta & Roy (1987) and Watson, Barnes & Peregrine (1994) have made comparisons of the solutions of these equations with experiments with encouraging results.

Carrier & Greenspan (1958) give an analytical solution for the shallow water motion of temporally periodic, finite-amplitude, non-breaking standing waves on a beach of constant slope. It is still one of the few analytic solutions available, together with that discovered by Shen & Meyer (1963) for run-up due to a bore. In §2 we analyse some

properties of the analytical solution of the nonlinear shallow water equations given by Carrier & Greenspan (1958). We also show that an analytic solution is possible for a weakly three-dimensional extension of their solution which builds on the work of Ryrie (1983). Results for some flow properties are given in the form of contour plots. In §3 some possible definitions of mean shoreline are given, and various flow properties are discussed. In §4 a model for integrated flow properties in the swash zone is described. This model enables computation of integral flow properties by using local flow quantities at the seaward limit of the swash zone. In §5 we discuss the application of the model equations to some test cases. Time series of the integral properties adopted to model the swash zone flow are illustrated and discussed. In §6 we show an example of how swash flow can be predicted from properties at the seaward limit of the swash zone.

The above-mentioned topics are all steps on the way to the main aim of this paper which is to derive swash zone boundary conditions suitable for wave-averaged models of the near-coastal area. We need to assume that the waves incident at the edge of the swash zone are divisible into long and short waves, and we average over the latter. The derivation of boundary conditions in §7 makes no further assumptions. Although we give a brief discussion in §8 of some of the averaged terms, using the full numerical solution, the present work is limited to providing the foundation on which further closure hypotheses can be made for practical implementations of surf and swash zone modelling.

2. An analytic solution of the shallow water equations

In this section we introduce the basic equations used to describe the flow dynamics near the shore. We also discuss an analytic solution of the equations valid for weakly three-dimensional flow conditions.

Motion of water waves near the shoreline on a gently sloping beach is described by many authors using various hydrodynamical equations: linear and nonlinear shallow water equations, Boussinesq equations and various related approximations. Stoker (1947) and Whitham (1979) describe exact solutions of the linearized shallow water equations on beaches of uniform slope for certain beach angles initially discovered by Hanson (1926). A long-wave approximation for the full equations of motion gives as the leading terms (see Peregrine 1972) the nonlinear shallow water equations (NLSWE). These equations are obtained by assuming that vertical accelerations of the water, or those normal to the beach, are negligible compared with gravity. Since no dispersive terms are included in the nonlinear shallow water equations, solutions for sufficiently steep waves travelling shoreward continually steepen and a bore, or jump, is inserted to represent breaking as the gradients become singular. Shallow water equations are used when motion is continuous, but across the discontinuity of height and velocity at the bore, or jump, mass, and momentum must be conserved (Hibberd & Peregrine 1979).

We introduce basic definitions, see figure 1, choosing the still water level to be $z = 0$ and the total water depth

$$d(x, y, t) = h(x) + \eta(x, y, t) \tag{2.1}$$

where $z = -h(x)$ is the seabed, $z = \eta(x, y, t)$ is the position of the free surface and y is in the longshore direction. The onshore and longshore velocity components, $u(x, y, t)$ and $v(x, y, t)$ are the depth-independent horizontal velocities used in the nonlinear shallow water equations (NLSWE).

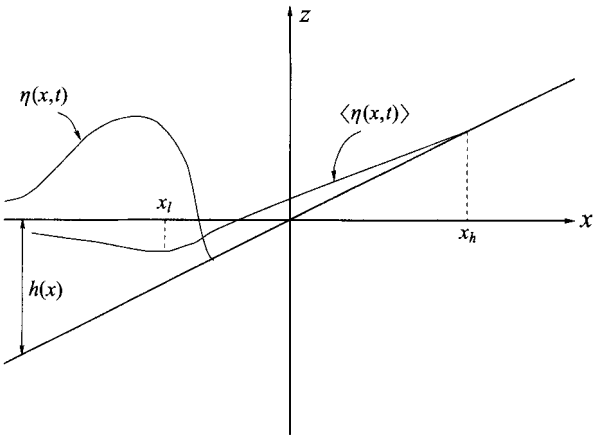

FIGURE 1. Surface definition in the vicinity of the swash zone.

For a plane beach the equations without bottom friction can be put in a simple dimensionless form with no explicit dependence on the beach slope α (Meyer & Taylor 1972; Hibberd & Peregrine 1979). The dimensional set of equations is

$$d^*_{t^*} + (d^*u^*)_{x^*} + (d^*v^*)_{y^*} = 0, \tag{2.2a}$$

$$u^*_{t^*} + u^*u^*_{x^*} + v^*u^*_{y^*} + gd^*_{x^*} = -g\alpha, \tag{2.2b}$$

$$v^*_{t^*} + u^*v^*_{x^*} + v^*v^*_{y^*} + gd^*_{y^*} = 0. \tag{2.2c}$$

Dimensionless variables chosen to eliminate the beach slope α from the equations are

$$d = \frac{d^*}{\alpha l_0}, \quad u = \frac{u^*}{u_0}, \quad v = \frac{v^*}{u_0}, \tag{2.3a}$$

$$x = \frac{x^*}{l_0}, \quad y = \frac{y^*}{l_0}, \quad t = \frac{t^*}{t_0}, \tag{2.3b}$$

$$t_0 = \left(\frac{l_0}{g\alpha}\right)^{1/2}, \quad u_0 = (gl_0\alpha)^{1/2} \tag{2.3c}$$

where l_0 is a reference length which can be specified according to the particular problem under investigation. The equations become

$$d_t + (du)_x + (dv)_y = 0, \tag{2.4a}$$

$$u_t + uu_x + vu_y + d_x = -1, \tag{2.4b}$$

$$v_t + uv_x + vv_y + d_y = 0. \tag{2.4c}$$

Friction terms are not included for the analysis and most of the numerical modelling. Even at laboratory scale they are of secondary importance if beach slope is not too small. Watson *et al.* (1994) give a quantitative estimate of their importance. However, the energy dissipation of bores is included in the modelling as discontinuities.

Equations (2.4) can be further simplified by approximating for waves incident at small angle θ to the beach normal (Ryrie 1983). Since waves approaching a beach from deep water are, in most circumstances, refracted toward the shore so that θ is small, this restriction is not severe for a single incident wave train. We introduce a pseudotime t' and a small parameter ϵ such that

$$t' = t - \epsilon y. \tag{2.5}$$

With this as the only y-dependence, it implies we are assuming that the wave pattern has a longshore phase velocity of $1/\epsilon$. For example, this can occur for a regular train of waves incident towards the shore at an angle θ to the shore normal, with an offshore velocity c, where $\epsilon = \sin\theta/c$. This approach can be extended to any beach that like the plane beach has uniform topography in the longshore direction.

For a weakly three-dimensional flow the additional scaling

$$v' = \frac{v}{\epsilon}, \tag{2.6}$$

on substitution into the NLSWE (2.4), neglecting $O(\epsilon^2)$ terms and dropping primes, gives the set of equations:

$$d_t + (du)_x = 0, \tag{2.7a}$$

$$u_t + uu_x + d_x = -1, \tag{2.7b}$$

$$v_t + uv_x - d_t = 0. \tag{2.7c}$$

The last of the above set of hyperbolic equations is now decoupled from the first two. The v-component of the velocity does not appear in (2.7*a*,*b*) ('onshore problem') and a solution for (2.7*c*) ('longshore problem') is found once d and u are known. Characteristic directions in the (x,t)-plane for the system (2.7) are given for the onshore and longshore problem respectively by

$$\frac{\mathrm{d}x}{\mathrm{d}t} = u \pm c \quad \text{and} \quad \frac{\mathrm{d}x}{\mathrm{d}t} = u. \tag{2.8}$$

Equations (2.7) can be expressed in characteristic form with the Riemann invariants α, β and γ:

$$\alpha_t + (u+c)\alpha_x = 0, \tag{2.9a}$$

$$\beta_t + (u-c)\alpha_x = 0, \tag{2.9b}$$

$$\gamma_t + u\gamma_x = 0, \tag{2.9c}$$

where the Riemann invariants are defined as follows:

$$\alpha = 2c + u + t, \tag{2.10a}$$

$$\beta = 2c - u - t, \tag{2.10b}$$

$$\gamma = v - \tfrac{1}{2}u^2 - d - x = v - \tfrac{1}{2}u^2 - \eta. \tag{2.10c}$$

Carrier & Greenspan (1958) used a hodograph transformation in solving the onshore problem:

$$\lambda = \alpha - \beta = 2(u+t)\,, \quad \sigma = \alpha + \beta = 4c\,, \quad u(\sigma,\lambda) = \frac{\phi_\sigma}{\sigma}. \tag{2.11}$$

The characteristic coordinates (σ,λ) are particularly effective for the moving shoreline since the $\sigma = 0$ contour maps the moving shoreline $d = c = 0$. We can also see that σ is a space-like coordinate and λ is a time-like coordinate (e.g. see figure 2*a*): in the limit of either small wave amplitude or large values of σ a simple relationship holds:

$$(x,\ t) \approx (-\tfrac{1}{16}\sigma^2,\ \tfrac{1}{2}\lambda). \tag{2.12}$$

Combining the equations for the onshore problem gives a linear equation in ϕ:

$$(\sigma\phi_\sigma)_\sigma - \sigma\phi_{\lambda\lambda} = 0. \tag{2.13}$$

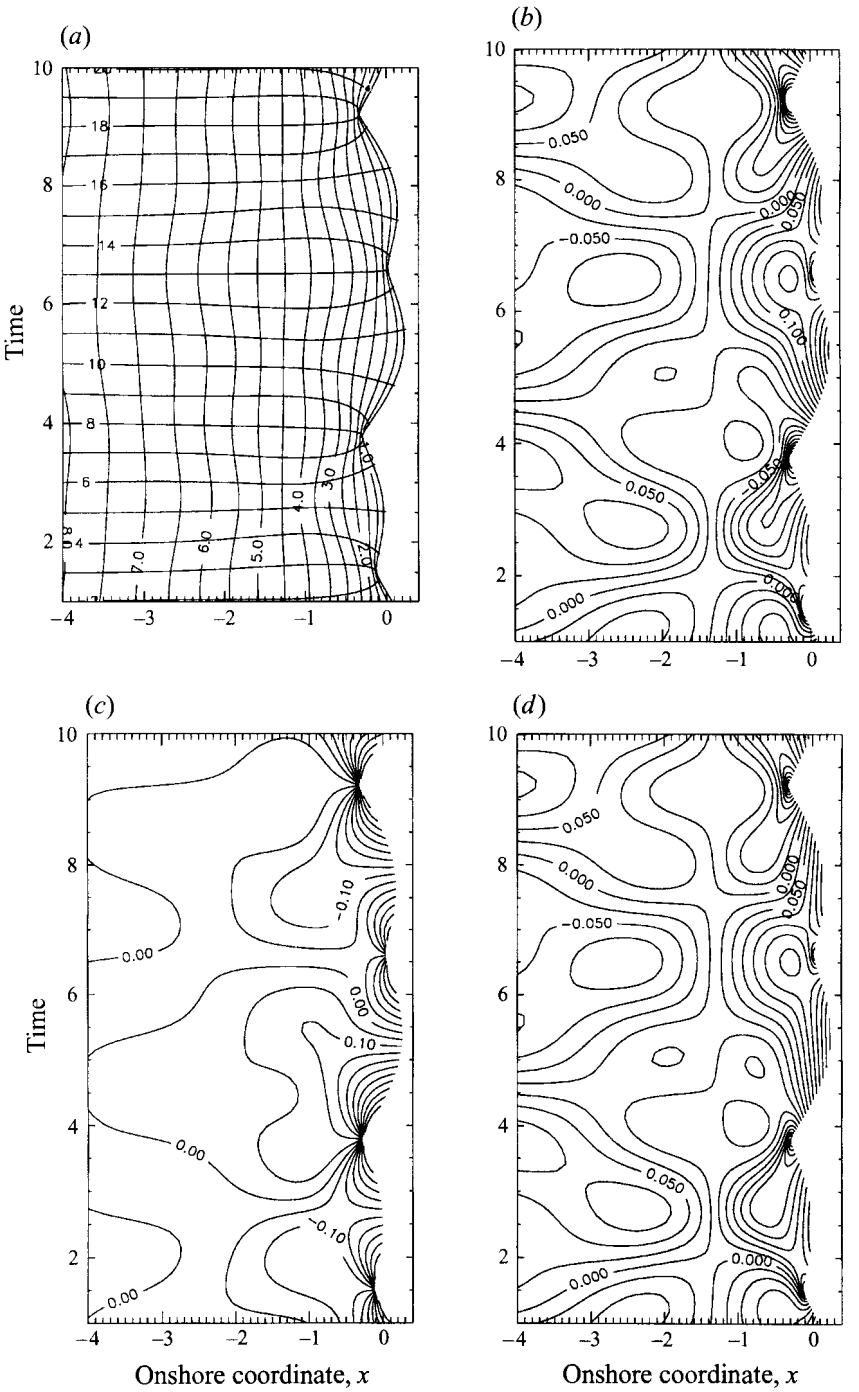

FIGURE 2. Superposition of two waves. Contour plots of: (*a*) the (σ, λ)-coordinates in the (x, t)-plane. Lines of constant λ run from left to right whilst lines of constant σ run from top to bottom. (*b*) The free surface elevation η, (*c*) the onshore velocity u and (*d*) the longshore velocity v. Dimensionless amplitudes and frequencies are $A_1 = 1.5$, $\omega_1 = 0.5$ and $A_2 = 0.5$, $\omega_2 = 1.2$ respectively.

The linearity of the above equation means its solution can be given as a sum of Fourier modes:

$$\phi(\sigma,\lambda)=\sum_{k=0}^{N}A_kJ_0(\omega_k\sigma)\sin\vartheta_k\ ,\quad \vartheta_k=\omega_k\lambda+\psi_k \tag{2.14}$$

where J_0 is the Bessel function of the first kind and which give explicit expressions for x,t,η,u once (2.9) are integrated (Carrier & Greenspan 1958; Synolakis 1987):

$$x(\sigma,\lambda)=\tfrac{1}{4}\phi_\lambda-\tfrac{1}{16}\sigma^2-\tfrac{1}{2}u^2, \tag{2.15a}$$

$$t(\sigma,\lambda)=\tfrac{1}{2}\lambda-u, \tag{2.15b}$$

$$\eta(\sigma,\lambda)=\tfrac{1}{4}\phi_\lambda-\tfrac{1}{2}u^2. \tag{2.15c}$$

Note that ω_k as defined in (2.14) is twice the frequency of waves where they are linear because of the factor 2 in the definition of λ, equation (2.11).

A two-mode example is illustrated in figure 2. However, not all the solutions can be transformed back to the (x,t)-plane. This problem occurs when the Jacobian of the transformation $(x,t)\rightarrow(\sigma,\lambda)$ vanishes. The transformation is only single valued when

$$\sum_{k=0}^{N}A_k\omega_k^3\cos\vartheta_k\leqslant 1. \tag{2.16}$$

Figure 2 shows an example of a two-mode solution obtained by superposing two modes for which condition (2.16) is satisfied. In order to show details, the solution is given for time shorter than the modulation period.

For a single-mode solution (2.14) is $\phi(\sigma,\lambda)=AJ_0(\omega\sigma)\sin\vartheta$, $\vartheta=\omega\lambda+\psi$ and equation (2.16) reduces to the simple condition $A\omega^3\leqslant 1$. This corresponds to a wave of amplitude A and frequency $\frac{1}{2}\omega$ travelling shoreward and being reflected out to sea generating a standing wave. This type of solution has been used in the past when analysing the dynamics of water waves approaching a coast or a continental shelf. Carrier (1966) matches both nonlinear shallow water theory and linear theory for deeper water to obtain a prediction of run-up for incident linear waves; also Keller (1963) and Carrier (1971) use the same solution when studying the dynamics of tsunamis.

Since the equation for the longshore problem is decoupled we can formally integrate equation (2.9*c*) once the Riemann invariant γ is substituted by its explicit expression:

$$0=\gamma_t+u\gamma_x=v_\lambda x_\sigma-v_\sigma x_\lambda+u(v_\sigma t_\lambda-v_\lambda t_\sigma)-(\eta_\lambda x_\sigma-\eta_\sigma x_\lambda). \tag{2.17}$$

After some algebra the equation can be rearranged to give

$$\left(\tfrac{1}{2}-\frac{\phi_{\sigma\lambda}}{\sigma}\right)\left(2v_\lambda-\frac{\phi_\sigma}{\sigma}\right)-\tfrac{1}{2}\left(\phi_{\sigma\sigma}-\frac{\phi_\sigma}{\sigma}\right)\left(\tfrac{1}{2}-4v_\sigma\right)=0. \tag{2.18}$$

A solution valid for any ϕ is

$$v=\tfrac{1}{4}\phi_\lambda+\text{const.} \tag{2.19}$$

and setting const. $=0$ we get

$$v=\tfrac{1}{4}\sum_{k=0}^{N}A_k\omega_kJ_0(\omega_k\sigma)\cos\vartheta_k. \tag{2.20}$$

Contour plots of the free surface elevation and velocity components help visualize

the behaviour of the solution, see figures 2 and 3 for superposition of two modes, and for a single mode respectively. The multimodal solution is less general than it looks since it still has the requirement of constant longshore phase velocity. In that respect it could be useful for modelling the waves generated by a ship moving at constant speed parallel to the shoreline, an important consideration for canals, rivers and navigation channels where shore erosion is often a major problem.

For all the flow properties of the single-mode solution shown in figure 3 there is a cell-structured pattern. Cells are confined by surface contours of zero level; they also have different sizes and shapes. For all of them the largest values are reached within the most onshore cell. The particular characteristic of the contour structure for u is that it has an antisymmetric cellular pattern within the period. We can therefore state *a priori* that its mean value over a wave period is zero at each $x = \text{const.}$ position. This is not true for either the free surface elevation or the longshore velocity. They have similar cell patterns and, for both of them, time averaging over a wave period results in a non-zero contribution.

3. The mean shorelines, and longshore flow

We now focus on the analysis of the flow near to the shoreline boundary of the domain where the single-mode solution obtained in the previous section is defined. In particular we describe swash zone flows with particular emphasis on mean flow properties, and note that a mean shoreline boundary is not uniquely defined. From analysis of available literature it seems clear that there is no unique definition for the mean shoreline, e.g. at one extreme Nielsen (1989) defines the mean shoreline as the maximum of the run-up. This is the result obtained from averaging the depth over the phase. On the other hand the mean position of the shoreline is an obvious definition.

We give several possible definitions of mean shoreline, each of a different character. The definitions are based either on kinematic flow properties (i.e. time or phase average of the waterline position), or on dynamic flow properties of the swash zone (i.e. involving mass or momentum fluxes) and a graphical representation of them is given in figure 4.

We illustrate some possible definitions by using the Carrier & Greenspan solution. Equations (2.14) and (2.15) give the single-mode solution

$$x = \tfrac{1}{4}\phi_\lambda - \tfrac{1}{16}\sigma^2 - \tfrac{1}{2}u^2 = \tfrac{1}{4}A\omega J_0(\omega\sigma)\cos\vartheta - \tfrac{1}{16}\sigma^2 - \frac{A^2\omega^2 J_1^2(\omega\sigma)\sin^2\vartheta}{2\sigma^2}\,, \tag{3.1a}$$

$$t = \tfrac{1}{2}\lambda - u = \tfrac{1}{2}\lambda + \frac{A\omega J_1(\omega\sigma)\sin\vartheta}{\sigma}. \tag{3.1b}$$

The moving shoreline is defined at $\sigma = 0$ and hence given by

$$x_s = \tfrac{1}{4}A\omega\cos\vartheta - \tfrac{1}{8}A^2\omega^4\sin^2\vartheta\,, \tag{3.2a}$$

$$t_s = \tfrac{1}{2}\left(1 + A\omega^2\sin\vartheta\right). \tag{3.2b}$$

The maximum and minimum positions of the shoreline are symmetric with respect to the still water level

$$x_{s_{Min}} = -\tfrac{1}{4}A\omega\,, \qquad x_{s_{Max}} = \tfrac{1}{4}A\omega = x_1. \tag{3.3}$$

Therefore x_1 represents the definition of Nielsen (1989). For this shoreline the mean water depth is zero.

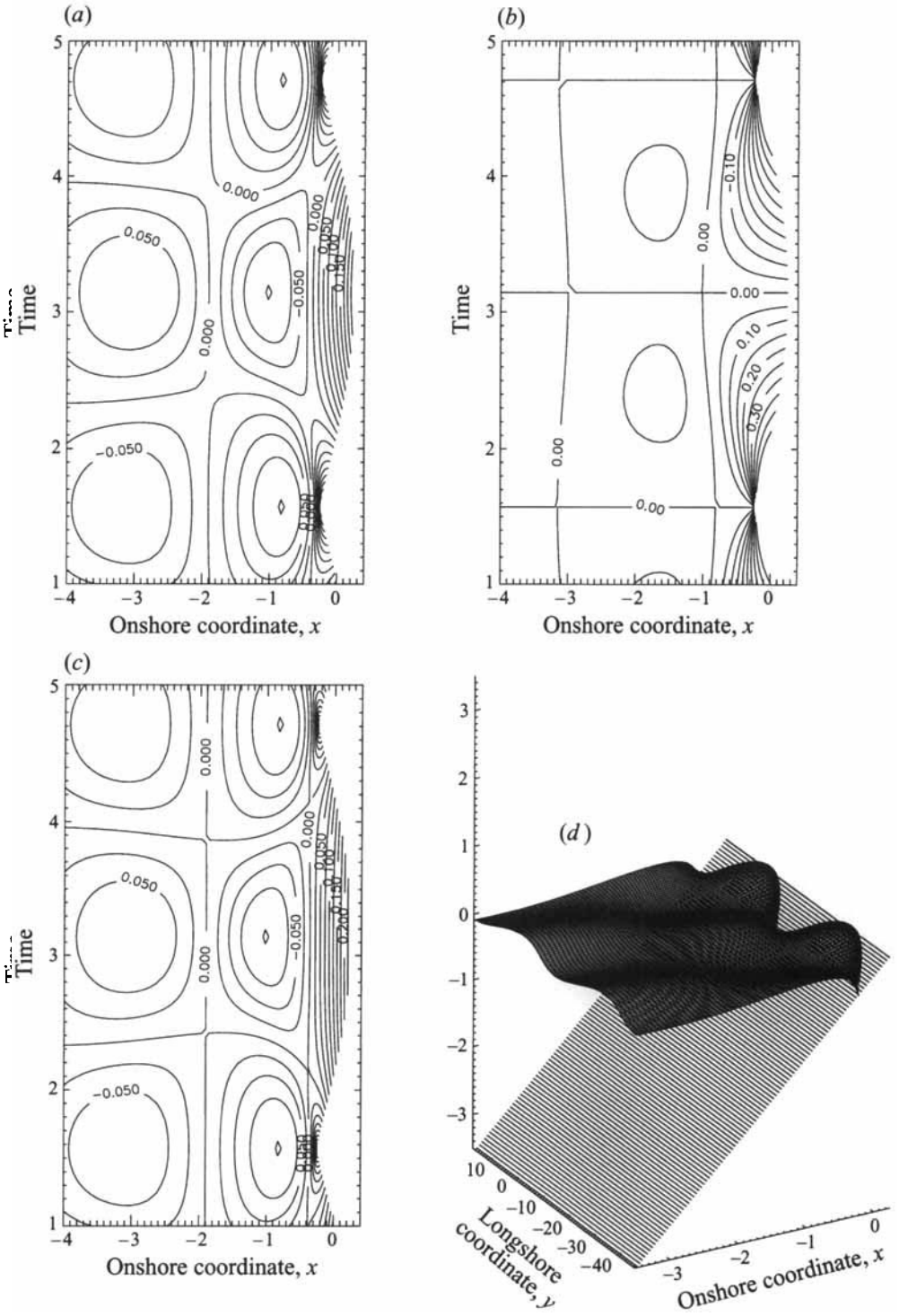

FIGURE 3. Contour lines of: (*a*) the free surface elevation, (*b*) the onshore velocity component u and (*c*) the longshore velocity component v in the (x,t)-plane. (*d*) Graphic image of the Carrier & Greenspan wave on the beach in dimensionless, scaled, coordinates. Dimensionless wave amplitude $A = 1$ and dimensionless wave frequency $\omega = 1$.

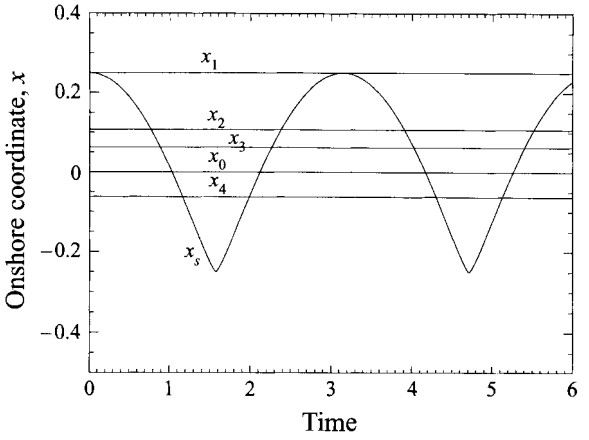

FIGURE 4. Some definitions for a mean shoreline for the Carrier & Greenspan solution with $A = \omega = 1$: x_0 = location of the still water level; x_1 = location of the wave maximum run up; x_2 = median shoreline i.e. location where wet and dry alternates for equal time during a wave cycle; x_3 = mean shoreline i.e. time average of the actual shoreline x_s; x_4 = mean shoreline based on considerations on the longshore mass flux.

The obvious definition of mean shoreline is based on the phase average of the waterline position,

$$x_3 = \langle x_s \rangle = \frac{1}{T}\int_T x_s \, \mathrm{d}t = \frac{\omega}{\pi}\int_{-\pi/2\omega}^{\pi/2\omega} \left(\tfrac{1}{4}A\omega\cos\vartheta - \tfrac{1}{8}A^2\omega^4\sin\vartheta\right) \mathrm{d}t, \tag{3.4}$$

where $\langle\cdot\rangle$ is a wave average operator. At the waterline $\sigma = 0$ and therefore the time coordinate $t = t_s$ only depends on λ and a change of variable $t \to \lambda$ gives

$$x_3 = \frac{\omega}{2\pi}\int_{-\pi/2\omega}^{\pi/2\omega} \left(\tfrac{1}{4}A\omega\cos\vartheta - \tfrac{1}{8}A^2\omega^4\sin\vartheta\right)\left(A\omega^3\cos\vartheta + 1\right) \mathrm{d}\lambda = \tfrac{1}{16}A^2\omega^4. \tag{3.5}$$

Two other possible positions for a mean shoreline are shown. One is for the mean (median) shoreline x_2 such that wet and dry alternate for equal time during a wave cycle:

$$x_2 = \tfrac{1}{4}A\omega\cos\vartheta_2 - \tfrac{1}{8}A^2\omega^4\sin^2\vartheta_2\,, \tag{3.6a}$$

where ϑ_2 satisfies

$$2\omega(\lambda + A\omega^2\cos\vartheta_2) = \pm(2n+1)\pi \quad n \in \mathbb{N}, \tag{3.6b}$$

and the other for the shoreline x_4 such that the longshore mass flux in the swash zone is equal shoreward and landward of it:

$$\int_{-A\omega/4}^{x_4} \langle vd \rangle \, \mathrm{d}x = \int_{x_4}^{A\omega/4} \langle vd \rangle \, \mathrm{d}x. \tag{3.7}$$

It can be shown that the following holds:

$$x_1 > x_2\,, x_3\,, x_4\,; \quad x_2 > x_4\,, \quad \forall\, A, \omega \quad \text{such that} \quad 0 \leqslant A\omega^3 \leqslant 1. \tag{3.8}$$

In fact the function $\langle vd \rangle$ reaches its maximum value near the middle of the swash but seaward of the still water level position, i.e. $-A\omega/4 \leqslant x \leqslant 0$ (see figure 6).

Before considering averaging further we wish to clarify the relationships between the flow properties obtained from the dimensionless solution and their dimensional

	Dimensionless representation	
	$\omega = 1$	$A = 1$
Solution	$\phi(\sigma,\lambda) = AJ_0(\sigma)\sin\lambda$	$\phi(\sigma,\lambda) = J_0(\omega\sigma)\sin\omega\lambda$
Length scale	$l_0 = \dfrac{4g\alpha}{\omega^{*2}}$	$l_0 = 4\left(\dfrac{A^{*2}g}{\omega^{*2}\alpha}\right)^{1/3}$
Relation to run-up amplitude	$A = \dfrac{4A^*}{\alpha l_0} = \dfrac{A^*\omega^{*2}}{g\alpha^2}$	$\omega = \frac{1}{2}\omega^*\left(\dfrac{l_0}{g\alpha}\right)^{1/2} = \left(\dfrac{A^*\omega^{*2}}{g\alpha^2}\right)^{1/3}$

TABLE 1. Summary of solution form, length scale and complementary dimensionless variable for the two dimensionless representations of a single-Fourier-component Carrier & Greenspan solution.

counterparts. The single-mode solution is formally characterized by the three degrees of freedom associated with the dimensionless wave amplitude A, the dimensionless wave frequency ω and the phase shift ψ. The last variable can be set to zero when dealing with a single-wave mode by suitable choice of the time origin. Either of the two remaining parameters, A and ω, may be set equal to unity, without loss of generality, by suitable choice of the length scale l_0 used to make the equations (2.4) dimensionless, e.g. Carrier & Greenspan (1958) set $\omega = 1$. Table 1 shows the relationship between the two natural choices.

From (3.1*b*) and (2.3*c*) the dimensional frequency of any given wave is

$$\omega^* = 2\omega\left(\frac{g\alpha}{l_0}\right)^{1/2}. \tag{3.9}$$

On the other hand the dimensional amplitude A^* can be linked to the dimensionless parameters by inspection of the run-up height from equation (3.3):

$$-\tfrac{1}{4}A\omega \leqslant h \leqslant \tfrac{1}{4}A\omega \quad \Longrightarrow \quad -\tfrac{1}{4}A\omega\alpha l_0 \leqslant h^* \leqslant \tfrac{1}{4}A\omega\alpha l_0. \tag{3.10}$$

We can also link the dimensionless parameters to the deep water dimensional amplitude A^*_{Deep}. The run-up height can be obtained from the deep water amplitude through an amplification factor characteristic of linear small-amplitude theory (Keller 1961; Meyer & Taylor 1972):

$$\frac{A^*}{A^*_{Deep}} = \left(\frac{2\pi}{\alpha}\right)^{1/2}. \tag{3.11}$$

As a consequence of equation (3.10) we choose to define the dimensional amplitude as the run-up amplitude:

$$A^* = \tfrac{1}{4}A\omega\alpha l_0. \tag{3.12}$$

Requiring either $\omega = 1$ or $A = 1$ the length scale l_0 is set from equations (3.9) and (3.12) and its values are reported in table 1.

It is evident that the breaking condition expressed in dimensionless variables from (2.16) becomes in dimensional variables and for a single-mode solution

$$B = \frac{A^*\omega^{*2}}{g\alpha^2} \geqslant 1, \tag{3.13}$$

where the breaking parameter B is widely used in coastal engineering to assess

both the incipient wave breaking over a slope and also to distinguish between the qualitatively different types of breaking (see Galvin 1972). For many of the figures we choose $\omega = 1$, but report analytical results with general A and ω.

Time averaging of flow properties is rather involved for the Carrier & Greenspan solution because of difficulties in relating (x,t) and (σ,λ). Let

$$\langle G(x,t)\rangle = \frac{1}{T}\int_T G(x,t)\,\mathrm{d}t = \frac{1}{T}\lim_{t\to T} H(x,t) \tag{3.14}$$

be the time average of $G(x,t) = g(\sigma,\lambda)$ where

$$H(x,t) = \int_0^t G(x,s)\,\mathrm{d}s. \tag{3.15}$$

To evaluate this type of average which is based on time integration on curves of $x = \text{const.}$ we solve the following partial differential equation along the curves $x = \text{const.}$ in the (σ,λ)-plane:

$$\frac{\partial H}{\partial t} = G(x,t) = g(\sigma,\lambda). \tag{3.16}$$

But for constant x we have

$$\frac{\mathrm{d}H}{\mathrm{d}\lambda} = \frac{\partial H}{\partial t}\left(\frac{\partial t}{\partial \sigma}\frac{\mathrm{d}\sigma}{\mathrm{d}\lambda} + \frac{\partial t}{\partial \lambda}\right). \tag{3.17}$$

From these equations a set of two ordinary differential equations for $\langle G(x,t)\rangle$ and σ is obtained:

$$\left.\begin{aligned} \frac{\mathrm{d}\langle G(x,t)\rangle}{\mathrm{d}\lambda} &= \frac{1}{T}\lim_{t\to T} g(\sigma,\lambda)\left[\frac{\partial t}{\partial \lambda}\left(-\frac{\partial x}{\partial \lambda}\Big/\frac{\partial x}{\partial \sigma}\right) + \frac{\partial t}{\partial \sigma}\right] \\ \frac{\mathrm{d}\sigma}{\mathrm{d}\lambda} &= -\frac{\partial x}{\partial \lambda}\Big/\frac{\partial x}{\partial \sigma}. \end{aligned}\right\} \tag{3.18}$$

The first equation is the total derivative of $\langle G(x,t)\rangle$ in terms of $G(x,t)$ while the second states that we are integrating along curves where $x = \text{const.}$ This method is used to compute the time average of velocities and mass fluxes.

A first interesting result is obtained for the mean longshore velocity: a mean drift is associated with the swash zone width while the average is identically zero outside the swash zone (see figure 5). This closely resembles what happens for the Stokes' drift where a mass flux is associated with the motion of the free surface, with zero mass flux below the trough level, and hence is expected. However a more interesting result relates to the mean longshore mass flux (see figure 6). Correlation between solutions for the total water depth and the longshore velocity is such that the mean longshore mass flux is non-zero for a wide range of the solution domain. Even though the mean longshore mass flux is an order of magnitude smaller than the mean longshore velocity, mass transport effects are also non-negligible outside the swash zone.

At any point in the swash zone the mean water depth $\langle d\rangle$ is non-zero except at the upper limit. In figure 7 the mean free surface elevation and the position of the mean shoreline $x_3 = A^2\omega^4/16$ are shown. The mean water depth at this shoreline, x_3, is shown in figure 8 as a function of amplitude A. Note that even if there is no breaking a set-up still occurs at the antinode of this standing wave.

Choosing any mean shoreline for which the mean water depth is non-zero affects the definition of boundary conditions at the mean shoreline for the mean flow motion.

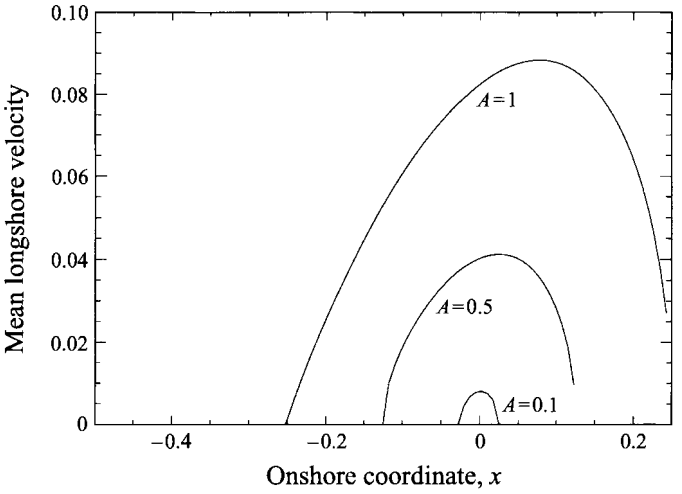

FIGURE 5. Mean longshore velocity in the swash zone for $A = 1$, $A = 0.5$ and $A = 0.1$ ($\omega = 1$ for all the cases). The seaward limit of the swash zone is given by the intersection of the curves and the x-axis.

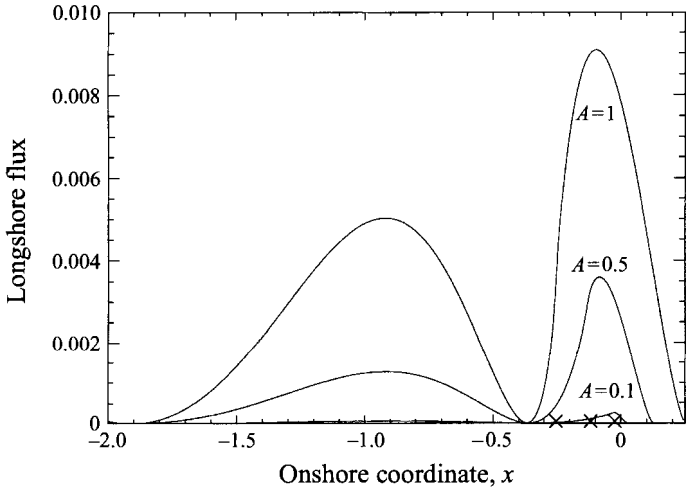

FIGURE 6. Mean longshore mass flux inside and near to the swash zone for $A = 1$, $A = 0.5$ and $A = 0.1$ ($\omega = 1$ for all the cases). The seaward limit of the swash zone is represented by a $\times$ symbol.

Conditions for absorption of water volume and onshore momentum are required. Within the swash zone the geometry of the slope affects the averaging methods, hence the difficulty in obtaining boundary conditions at the mean shoreline. In the next section we show how it is possible to circumvent problems in defining boundary conditions at the mean shoreline by obtaining boundary conditions at the seaward boundary of the swash zone.

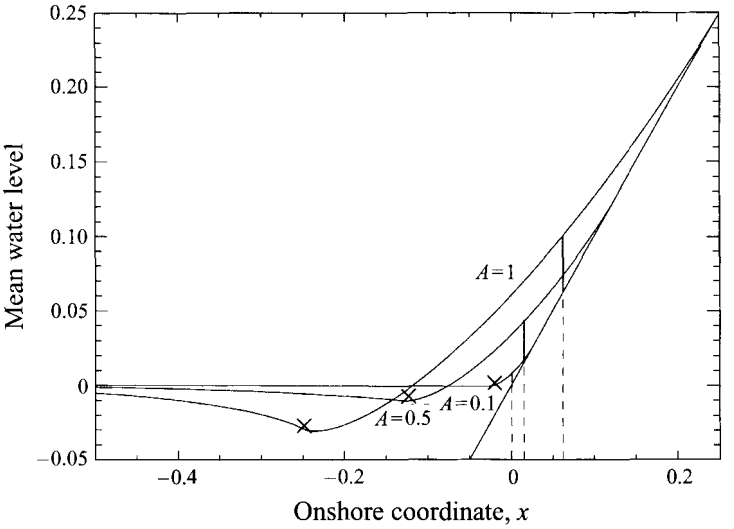

FIGURE 7. Mean free surface water level near to the swash zone for $A = 1$, $A = 0.5$ and $A = 0.1$ ($\omega = 1$ for all the cases). The seaward limit of the swash zone is represented by a $\times$ symbol.

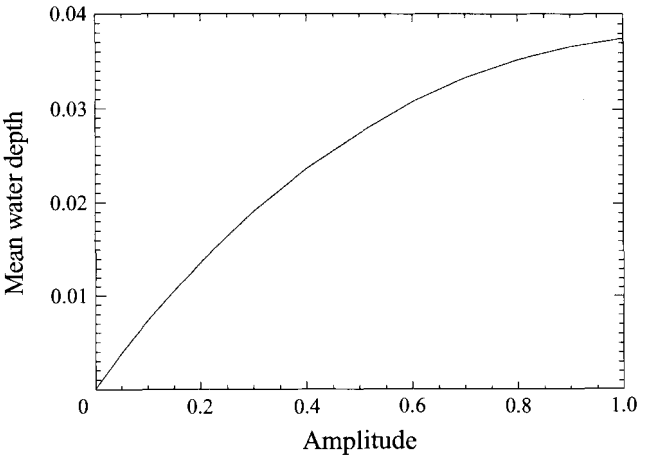

FIGURE 8. Mean water depth $\langle d \rangle$ at the mean shoreline x_3.

4. Integrated flow properties in the swash zone

When the NLSWE are integrated numerically for the surf and swash zone, it is the swash zone that proves to be the most demanding in terms of resolution for accurate integration. It would be helpful for many wave-resolving integrations if the swash zone were to be replaced by a simplified model. Here we present the direct results of integrating across the swash zone, and in the following section investigate the accuracy of this simplification.

In averaging across the swash zone it is not clear what is the best way to proceed, since no previous studies have been found. We follow by analogy an approach used by Svendsen & Lorenz (1989), Svendsen & Putrevu (1994) and others for dealing with the moving free surface in order to average flow properties in the surf zone by treating the region above the trough level as a distinct region, that is we investigate a model with a boundary chosen at the lower limit of the swash zone.

The swash zone limits are x_l , x_h, the seaward (lower) and shoreward (higher) limits of the swash zone respectively. The seaward boundary may, for example, be the lowest limit x_l of the moving shoreline in a group of waves. Integral properties of the water shoreward of that point are considered.

We integrate the basic flow equations across the swash zone. In the following we adopt Einstein's summation convention and use Greek suffices for the two-dimensional horizontal flow properties. The general set of equations (2.4) is put in conservation form:

$$d_t + (ud)_x + (vd)_y = 0, \tag{4.1a}$$

$$(ud)_t + \left(u^2 d + \tfrac{1}{2}d^2\right)_x + (uvd)_y + d + \tau_1 = 0, \tag{4.1b}$$

$$(vd)_t + (uvd)_x + \left(v^2 d + \tfrac{1}{2}d^2\right)_y + \tau_2 = 0, \tag{4.1c}$$

$$\tfrac{1}{2}\left[d(u^2+v^2) + d^2\right]_t + \left(\tfrac{1}{2}u^3 d + \tfrac{1}{2}v^2 ud + ud^2\right)_x + \left(\tfrac{1}{2}v^3 d + \tfrac{1}{2}u^2 vd + vd^2\right)_y + u(d+\tau_1) + v\tau_2 = 0, \tag{4.1d}$$

where a dimensionless bed friction $\boldsymbol{\tau} = (\tau_1, \tau_2)$ and the energy equation are included.

Before integrating the above equations over the swash zone width we make an assumption concerning the time scales of the wave motion and of the motion of the swash zone boundary. We consider the wave motion as occurring on a 'fast time scale' t while the swash zone boundaries x_h (run-up) and x_l (run-down) are supposed to vary (if varying in time) on a 'slow time scale' T such as $t = \epsilon T$. (We do not use this explicit notation since the separation of the two scales is generally quite clear.) We can identify the 'fast time scale' t with the typical period of each single incident wave. On the other hand the 'slow time scale' T might be identified with the typical period of modulations of incident short waves. With this definition we can identify the short-period motions with the wave motion on the time scale of the single wave while long-period motions are all those motions, both waves and currents, occurring with a period longer than T. Initially, in this and the next two sections, we mantain a constant value for x_l.

Equations (4.1) are integrated over the swash zone width for constant x_l, to give

$$\frac{\partial V}{\partial t} = \int_{x_l}^{x_h} d_t \, \mathrm{d}x = Q_1(t)|_{x_l} - \frac{\partial P_2}{\partial y}, \tag{4.2a}$$

$$\frac{\partial P_1}{\partial t} = \int_{x_l}^{x_h} (ud)_t \, \mathrm{d}x = S_{11}(t)|_{x_l} - V(t) - \frac{\partial M_{12}}{\partial y} - \Upsilon_1(t), \tag{4.2b}$$

$$\frac{\partial P_2}{\partial t} = \int_{x_l}^{x_h} (vd)_t \, \mathrm{d}x = S_{12}(t)|_{x_l} - \frac{\partial M_{22}}{\partial y} - \Upsilon_2(t), \tag{4.2c}$$

$$\frac{\partial E}{\partial t} = \int_{x_l}^{x_h} [\tfrac{1}{2}(u^2+v^2)d + d^2]_t \, \mathrm{d}x \tag{4.2d}$$

$$= F(t)Q_1(t)|_{x_l} - P_1(t) - \frac{\partial}{\partial y}\int_{x_l}^{x_h} FQ_2 \, dx - \Gamma(t).$$

These equations introduce a number of new flow properties and flow properties integrated over the swash zone. These are listed in table 2 where $\boldsymbol{u} = (u_1, u_2)$ is the horizontal velocity vector.

The set of equations (4.2) for the fully three-dimensional motion can be reduced by Ryrie's approximation to a simpler set of equations valid for weakly three-dimensional motion. Second-order terms are neglected after the formal substitution (2.6) is made.

Name	Explicit expression	Flow property
Q_μ	$u_\mu d$	Local mass flow
$S_{\mu\nu}$	$u_\mu u_\nu d + \delta_{\mu\nu}\frac{1}{2}d^2$	Local momentum flux tensor
F	$\frac{1}{2}\boldsymbol{u}^2 + d$	Local energy density
V	$\int_{x_l}^{x_h} d\ \mathrm{d}x$	Volume of water in swash zone
P_μ	$\int_{x_l}^{x_h} Q_\mu\ \mathrm{d}x$	Momentum of water in swash zone
$M_{\mu\nu}$	$\int_{x_l}^{x_h} S_{\mu\nu}\ \mathrm{d}x$	Integrated momentum flux tensor
E	$\int_{x_l}^{x_h}(\frac{1}{2}\boldsymbol{u}^2 d + d^2)\ \mathrm{d}x$	Energy of water in swash zone
Υ_μ	$\int_{x_l}^{x_h} \tau_\mu\ \mathrm{d}x$	Friction force in swash zone
Γ	$\int_{x_l}^{x_h} u_\mu \tau_\mu\ \mathrm{d}x$	Work done by friction in swash zone

TABLE 2. Definition of the flow properties adopted in equations (4.2).

Name	Explicit expression	Flow property
$\bar{F}$	$\frac{1}{2}u_1^2 + d$	Local energy density
$\bar{E}$	$\int_{x_l}^{x_h}\frac{1}{2}(u_1^2 d + d^2)\ \mathrm{d}x$	Energy of water in swash zone
$\bar{\Gamma}$	$\int_{x_l}^{x_h} u_1\tau_1\ \mathrm{d}x$	Work done by friction in swash zone

TABLE 3. Definition of some flow properties adopted in equations (4.3).

Then, at the leading order the set of equations (4.2) becomes

$$\frac{\partial V}{\partial t} = \int_{x_l}^{x_h} d_t\ \mathrm{d}x = Q_1(t)|_{x_l}, \tag{4.3a}$$

$$\frac{\partial P_1}{\partial t} = \int_{x_l}^{x_h} (ud)_t\ \mathrm{d}x = S_{11}(t)|_{x_l} - V(t) - \Upsilon_1(t), \tag{4.3b}$$

$$\frac{\partial P_2}{\partial t} = \int_{x_l}^{x_h} (vd)_t\ \mathrm{d}x = S_{12}(t)|_{x_l} + \frac{\partial M_{22}}{\partial t} - \Upsilon_2(t), \tag{4.3c}$$

$$\frac{\partial \bar{E}}{\partial t} = \int_{x_l}^{x_h} (\tfrac{1}{2}u^2 d + d^2)_t\ \mathrm{d}x = \bar{F}(t)Q_1(t)|_{x_l} - P_1(t) - \bar{\Gamma}(t). \tag{4.3d}$$

Table 3 lists definitions which, because of the approximation, differ from those of table 2. We distinguish newly defined flow properties by using overbars in equations (4.3) and table 2.

In the idealized case of no dissipation ($\Upsilon_1 = \Upsilon_2 = \bar{\Gamma} = 0$), and no longshore variation, the set of partial differential equations (4.3) is such that it can be recursively solved for the integral flow properties in the swash zone (i.e. V, P_1, P_2 and $\bar{E}$) once the local flow properties Q_1, S_{11}, S_{12} and $\bar{F}$ are known at the seaward boundary of the swash zone. The equation for the water volume only depends on the known variable Q_1. Once this equation is solved for V the result can be substituted into the second equation and so on. This is illustrated in the next section. If the frictional terms were

suitably parametrized similar integration would be possible; however, for this initial analysis we consider only the frictionless case.

In deriving these equations (4.2) and (4.3) it is implicitly assumed that all the functions u, v, d are continuous solutions satisfying the NLSWE. This is not the case if a bore, represented by a discontinuity, is present within the swash zone. This presents no problem for the mass and momentum equations, but, as given in (4.2*d*) and (4.3*d*) no account has been taken of energy dissipated by a bore. For a strictly periodic swash zone, due to a single-mode wave, this is unimportant since x_l may be defined as the line on which each successive bore meets the shoreline. As a bore meets the shoreline its turbulent dissipation ceases, and only bed friction acts. Ho & Meyer (1962) describe this as the collapse of the bore. In unsteady flows bores are likely to travel for at least some distance inside the swash zone as we define it here. Although this behaviour is illustrated in the next section, it is relatively unimportant since the mass and momentum equations are sufficient for all necessary wave modelling.

5. Time variation of swash zone properties

In this section we discuss the application of the integrated swash zone equations of §4 to some typical test cases. The set of equations (4.3) is used rather than the full set (4.2) for three-dimensional motion since we have the analytic solution (2.20) for the longshore velocity in the case of weakly three-dimensional motion and it is also much easier to compute solutions for these equations. This can also be useful when dealing with phase-averaged equations where a model for the short-period wave motion must be given. We, thus, analyse in detail the results that can be obtained by the equations for weakly three-dimensional motion.

The main aim of the following discussion is to illustrate and to assess the effectiveness of the integral relationships for the analysis of the swash zone motion under as general flow conditions as possible. In particular for non-periodic waves each single run-down location does not coincide with the chosen seaward limit of the swash zone x_l. Thus the nominal swash zone may sometimes be noticeably larger than the swash of a single wave. Hence a number of examples have been computed, both with the integral relations (4.3) used at a fixed x_l and with full, numerical, solutions of equations (2.7). For the fully numerical solution the onshore and longshore problems are solved separately using the methods and numerical schemes given by Watson, Peregrine & Toro (1992) for the onshore problem and by Ryrie (1983) for the longshore problem.

Some features of real swash motion dynamics are introduced by using both uniform and modulated signals and including effects of wave breaking by allowing bore-like solutions to propagate towards the shore. This is achieved by setting the test input as follows. The seaward boundary of the numerical solution is set far enough from the bottom of the swash zone that the difference between the full solution and the linearized one is negligible. Here the shoreward propagating Riemann invariant obtained from the Carrier & Greenspan solution of period π, i.e. $\omega = 1$, is either used to generate a uniform train of periodic waves or is modulated with a long sinusoidal variation of amplitude $A(T)$ and period T ($T = 10\pi$ in our example) in order to give wave groups. By increasing the wave amplitude such that $A\omega^3 > 1$ we generate an input that propagates shoreward with bore formation, into a region which is initially at rest. Plots of time series for some of the quantities used to describe the swash zone dynamics are given in figures 9, 10 and 11. From figures 9 and 10 a comparison can be made of the order of magnitude of integral flow properties inside the swash zone with and without bore formation. While flow properties essentially depending

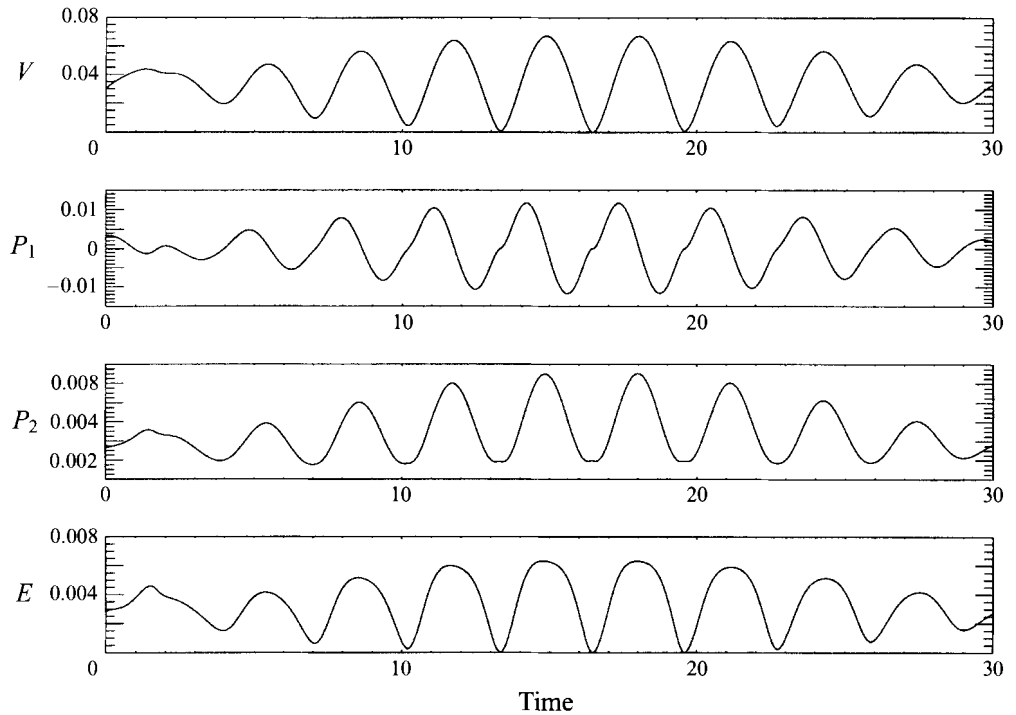

FIGURE 9. Model results for modulated Carrier & Greenspan type input of offshore amplitude $A = 1$ and frequency $\omega = 1$. No wave breaking occurs. Time series of volume, momentum and energy. Integrated quantities obtained from the numerical solution of the NLSWE.

on the onshore motion (V, P_1 and $\bar{E}$) are characterized by an increase of about 2 to 5 times when bores are present in the domain, a much larger increase of over two orders of magnitude occurs for the longshore momentum, P_2. This can be interpreted as evidence of the momentum transfer from waves to longshore currents due to wave breaking. The build-up of this larger flow is clearly evident.

Figure 11 is for a qualitatively different flow pattern from the previous two cases. At the seaward boundary uniform-amplitude input waves are incident on a region initially at rest. Periodic conditions at the shoreline are reached after an initial transient where run-up characteristics differ from those typical of run-up of non-interacting waves. There is an interval of time in which three bores are present simultaneously inside the swash zone. The space–time diagram in figure 12 helps clarify some details of this case where interaction of incoming bores and backwash motions occurs. The first bore meeting the still water shoreline does not encounter any resistance from backwash in the swash zone, hence its run-up is the largest. Subsequent bores, on the other hand, experience resistance from backwash due to previous run-up. In this particular case backwash of the first run-up is so strong it prevents the two following incoming bores meeting the shoreline. A third strong bore just inside the swash zone (see the arrow in figure 12) flows against the last, thin, high-speed portion of backwash which holds it at rest. This behaviour occurs while the inital transient conditions settle into a periodic solution. Once periodic conditions are reached very little dissipation occurs in the swash zone. However, observation, and other computations with random waves, show that this type of transient behaviour is not uncommon on a real beach.

For the two cases of modulated waves, breaking does not occur for the initial

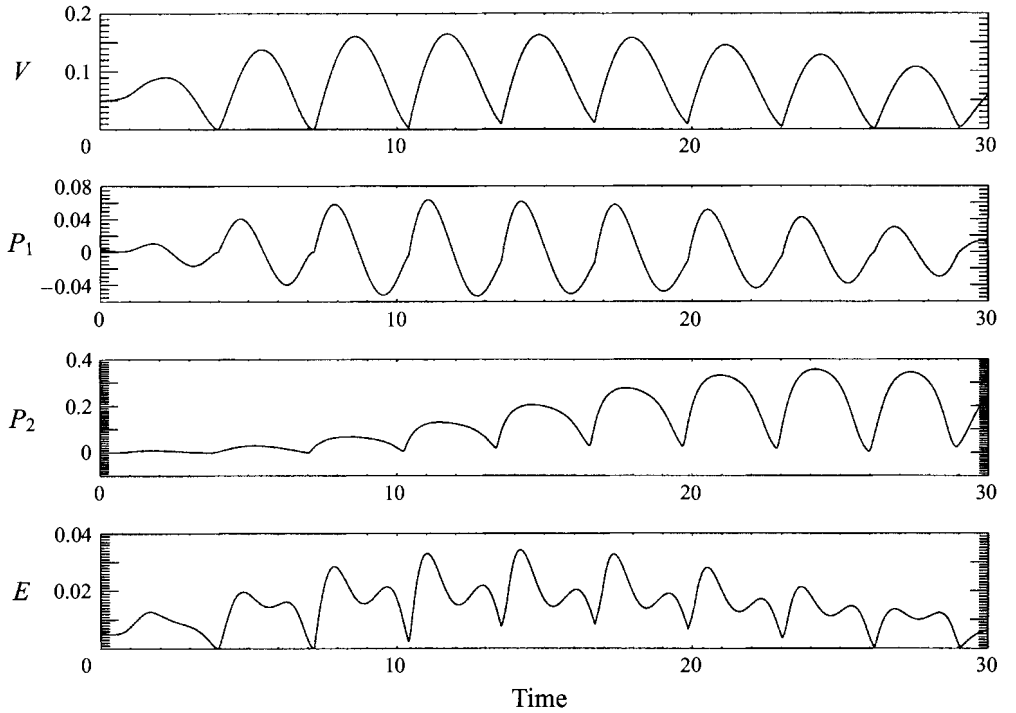

FIGURE 10. Model results for modulated Carrier & Greenspan type input of offshore amplitude $A = 5$ and frequency $\omega = 1$. Wave breaking occurs. Time series of volume, momentum and energy. Integrated quantities obtained from the numerical solution of the NLSWE.

smaller waves which hence contribute little to the longshore momentum, but larger waves undergoing full breaking greatly augment longshore momentum. It is also clear that when waves do not break effects of modulation are more evident for the longshore momentum P_2 than for the onshore momentum P_1 and energy $\bar{E}$. In fact modulation gives a slowly varying average to the signal of P_2 whereas for the others modulation is only present as time variation of the signal amplitude but the mean of the signal itself does not vary noticeably in time. On the other hand time modulation of the mean characterizes both $\bar{E}$ and P_2 once wave breaking occurs.

When one or more bores are in the swash zone, as defined by $x > x_l$, then the energy equation (4.3*d*) is expected to be in error. This is found to be the case when these equations are assessed numerically. Equations (4.3*a–c*) are found to be satisfactory within the anticipated numerical errors (the volume of water involved is often very small) for a wide range of flows, but as illustrated in figure 13 equation (4.3*d*) is of more limited value. The discrepancy between the actual rate of change of energy, the left-hand side of equation (4.3*d*) and the right-hand side of (4.3*d*) is shown in figure 13 together with a space-time diagram showing when bores are within $x > x_l$. This discrepancy is clearly associated with the time between a bore passing $x = x_l$ and the bore meeting the instantaneous shoreline.

The integrated swash zone equations (4.2*a–c*) and (4.3*a–c*) provide boundary conditions at $x = x_l$ for the waves in most of the surf zone. This should be of value for numerical integration, unless details of swash zone behaviour are required. When the full swash zone is included in a computation it not only involves a larger domain of integration with a special boundary condition at the shoreline, but also frequently determines the maximum permitted time-step. Hence, these integral representations

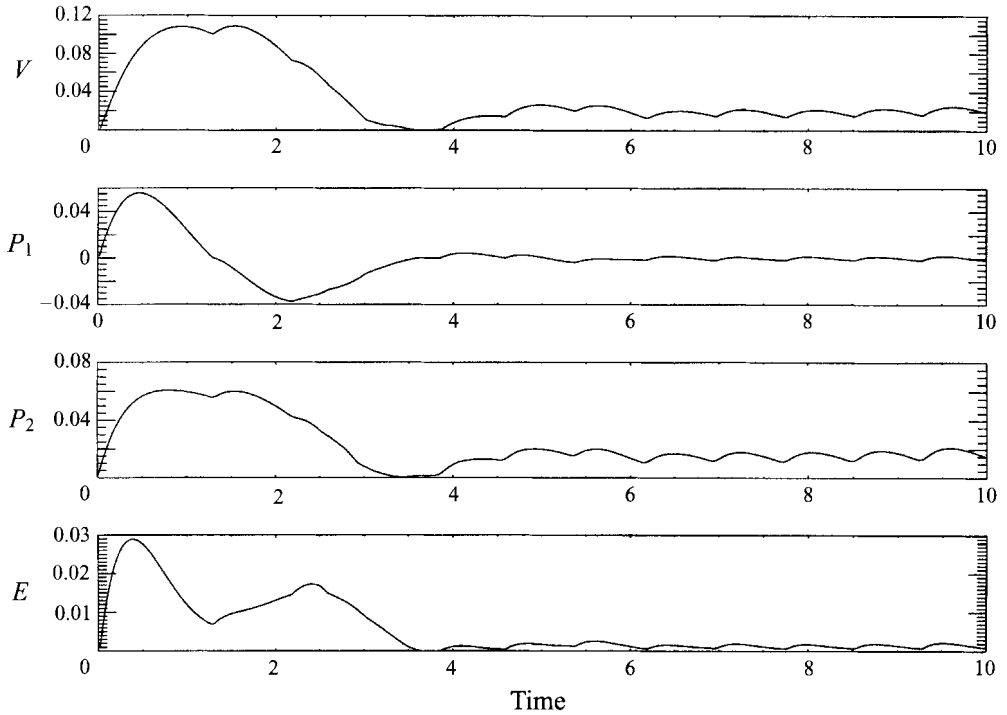

FIGURE 11. Model results for periodic Carrier & Greenspan type input of offshore amplitude $A = 8$ and frequency $\omega = 4$ starting from rest. Wave breaking occurs. Time series of volume, momentum and energy. Integrated quantities obtained from the numerical solution of the NLSWE.

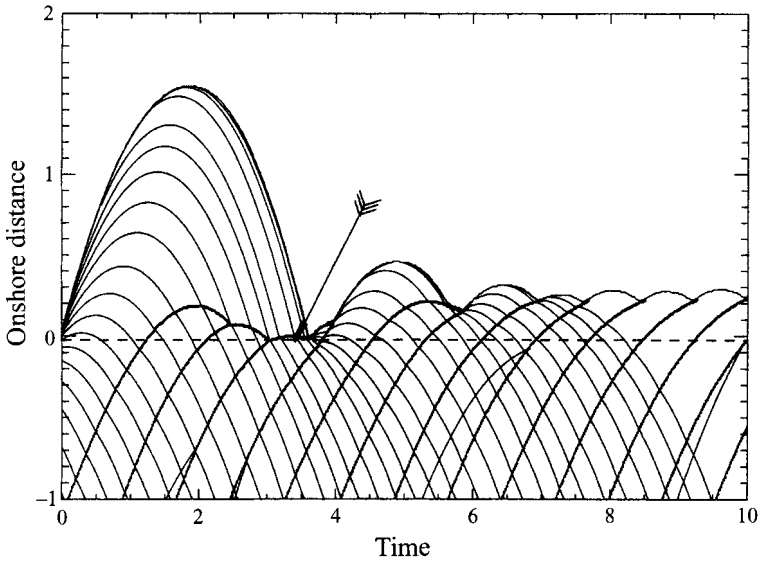

FIGURE 12. Model results for a periodic Carrier & Greenspan type input of offshore amplitude $A = 8$ and frequency $\omega = 4$ starting from rest. Wave breaking occurs. Characteristic curves, bore paths and shoreline are shown in the (x, t)-plane. The bore paths are represented by dotted lines, the broken line represents the seaward limit of the swash zone.

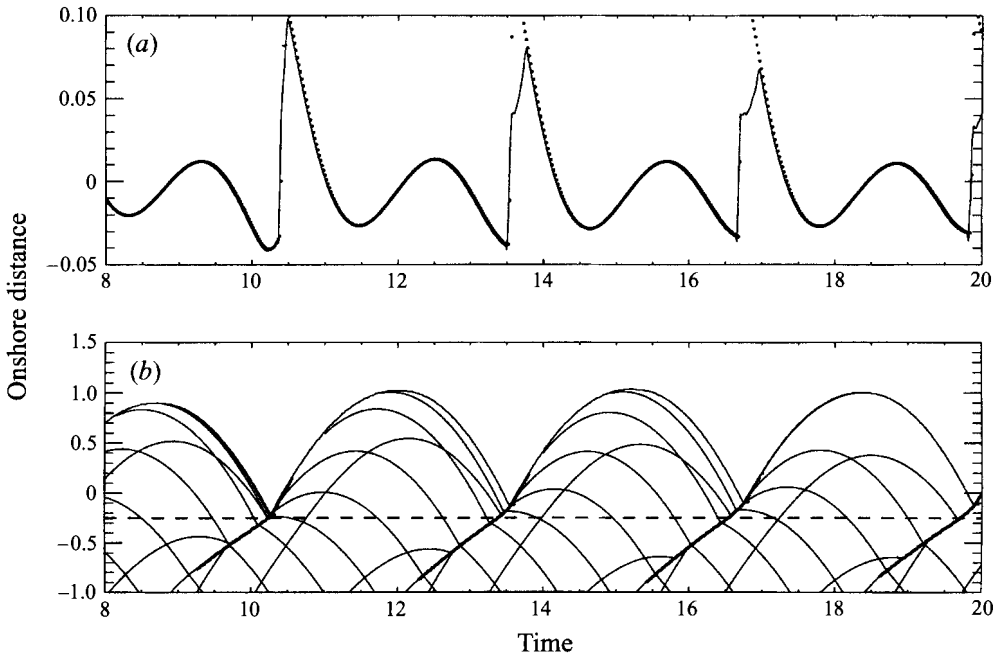

FIGURE 13. Model results for part of a modulated Carrier & Greenspan type input of offshore amplitude $A = 5$ and frequency $\omega = 1$. Wave breaking occurs. (*a*) Time series of the left-hand side (solid line) and right-hand side (thick dotted line) of equation (4.3*d*) as evaluated from a full numerical solution. (*b*) Characteristic curves, bore paths and shoreline in the (x, t)-plane. The bore paths are represented by thick dotted lines, the broken line represents the seaward limit of the swash zone.

may be useful, as well as representing one step towards the wave-averaged equations discussed in §7 and §8.

One limitation in the equations (4.2) and (4.3) is the omission of friction terms. These are deliberately omitted here so we are able to present results with no approximations beyond the NLSWE. If account is taken of friction, terms appear in the momentum and energy equations for which further closure approximations must be made. Such approximations are to be the subject of further study.

6. Swash flow from properties at x_l

To estimate swash zone flow properties from the integrated model we use simple geometric arguments based on water volume conservation to consider the inverse problem and estimate the moving shoreline. That is if Q, M etc. are known can we predict swash zone properties? The simplest approach assumes that the bulk of water running up and down in the swash zone is in the form of a triangular wedge. Both the base and the area of the triangle are known, being respectively the water depth d at the seaward limit of the swash zone and the total water volume V obtained from equations (4.3). The moving shoreline and other flow properites can therefore be estimated.

In figure 14 time series for both computed (thin line) and estimated (thick line) shorelines are shown for the modulated Carrier & Greenspan input signal of amplitude $A = 1$ and $A = 5$.

It is evident that while a satisfactory result is achieved in estimating the shoreline

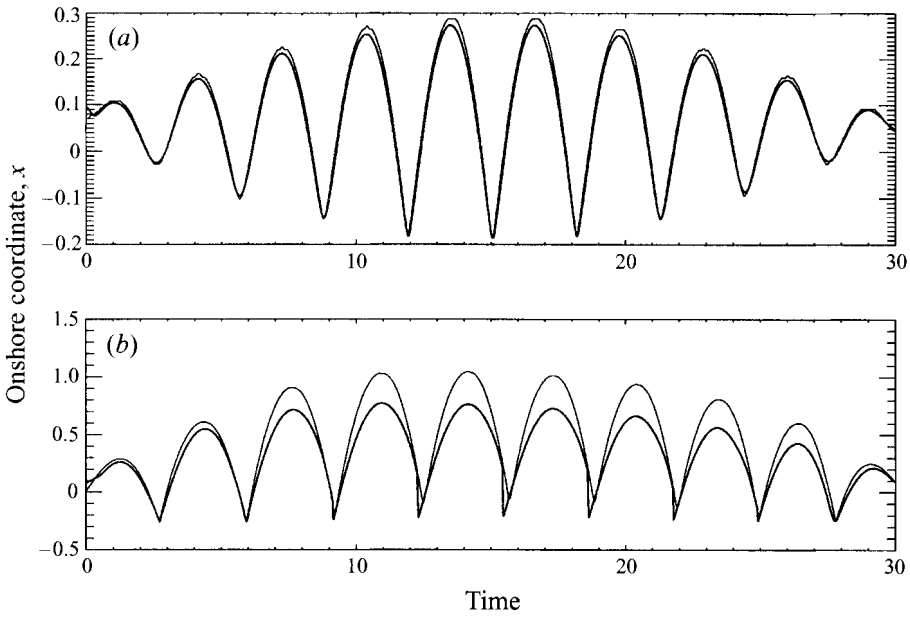

FIGURE 14. Computed and estimated shoreline for the modulated Carrier & Greenspan input signal of amplitude (*a*) $A = 1$ and (*b*) $A = 5$. Wave breaking occurs for the second case. Computed shorelines are drawn with a thin line while the estimate ones are given by a thick line.

when there is no breaking (case $A = 1$) this is not true when breaking is present (case $A = 5$) since the estimated shoreline underestimates the computed one. This is largely due to the different nature of shoreline motion when caused by a bore. As shown by Shen & Meyer (1963) the tip of the run-up due to a bore differs from that due to a smooth wave and has a quadratic variation of depth with distance from the instantaneous shoreline. This means that extremely thin sheets of water occur. Inclusion of any extra physical effect, such as bed friction, roughness, or surface tension can also lead to large differences in run-up position. Packwood (1980) has an example, here reproduced in figure 15, where comparison with a run-up meter illustrates this well. The computed shoreline is generally far from the measured shoreline. However the run-up gauge was insensitive to water depths of less than 2 mm, and reasonably good agreement is found for the 2 mm depth contour, for both inviscid computations and those including bed friction.

In similar fashion we also use the onshore momentum inside the swash zone (P_1) to estimate onshore velocity. The onshore velocity inside the swash zone is assumed to vary linearly from the boundary x_l to the estimated waterline. Computation has been performed for two modulated trains of amplitude $A = 1$ and $A = 5$. Comparison of the time series for P_1 reveals that no appreciable difference is found between the computed and estimated momentum when no wave-breaking occurs ($A = 1$ case). On the other hand some discrepancies appear when analysing the $A = 5$ case. They are more marked in the proximity of the extremal points (maxima and minima) of the time series. The largest discrepancy is detected near the maximum occurring at $t \approx 14$ (see figure 10) where the onshore momentum obtained from the numerical solution of the NLSWE is about 0.06. Here the percentage discrepancy is about 13%.

To illustrate the behaviour of the estimated (linear extrapolation) and computed onshore momentum inside the swash zone in more detail we compare the estimated

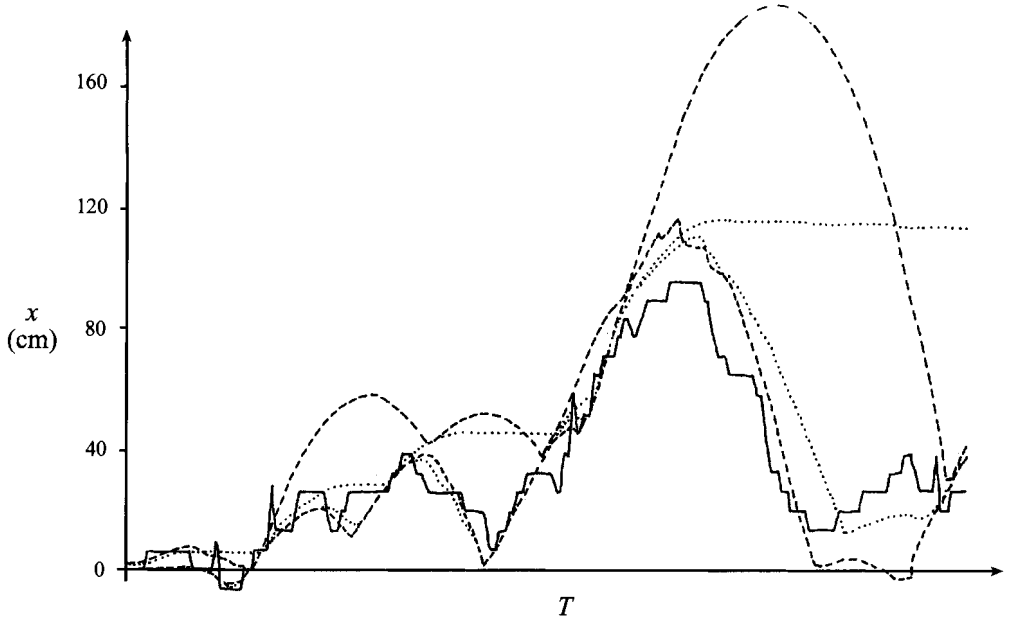

FIGURE 15. Comparison of computed and experimental run-up data from Packwood (1980) with permission of the author. Shoreline and 2 mm contours are shown for the computed solution. The experimental data (Hedges & Hawkes, private communication) from a run-up meter which was triggered by 2 mm water depth is drawn with a solid line, the data from the inviscid computed solution with a dashed line and the data from the computed solution including Chezy-type friction with a dotted line.

(dotted line) and computed (solid line) onshore velocity and water depth in the swash zone (see figure 16) at the time $t \approx 14$ when the largest discrepancy occurs. The largest errors in the estimated onshore velocity occur near the tip of the run-up, i.e. where the water depth becomes very small. The longshore velocity inside the swash zone can be suitably modelled by means of a linear profile which decreases from the breaking point to the shoreline. Ryrie (1983) reports results of computations which include friction and examples of linearly decreasing envelopes of maximum and minimum values of v across the entire surf zone are given. This and consideration of the difficulties in assessing and measuring water flow properties very close to the waterline suggest that computing flow properties by mean of the simplified model can give a reasonable estimate for most of the swash zone.

7. The swash zone boundary conditions for wave-averaged models

A natural extension to averaging the swash zone is to seek appropriate boundary conditions at the seaward swash zone limit for wave-averaged models of the incident motions (both long- and short-period motions). This requires definition of the contributions to the motion of the boundary $x = x_l$ from both long-period motions (e.g. low-frequency waves, currents, etc.) and averaged short-period motions. The problem here is that there is no definitive model for the waves approaching the swash zone, especially for the most usual case where waves are already breaking. The following discussion develops swash zone boundary conditions by assuming that appropriate short-wave properties are known. A brief illustration of some of these properties is given in the following section; however the main aim is to provide the foundation

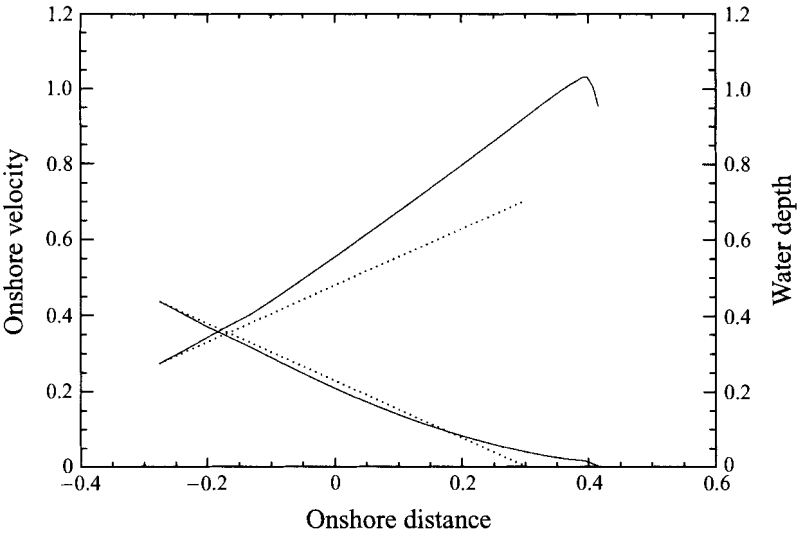

FIGURE 16. Computed (solid line) and estimated (dotted line) flow properties inside the swash zone for the modulated Carrier & Greenspan input signal of amplitude $A = 5$. The increasing curves represent the onshore velocity while the decreasing ones represent the water depth. (Note that the kink close to the shoreline is a computational artefact.)

from which further work may be developed, both in approximating the equations derived here and in improving the description of waves in the surf zone.

To obtain dynamic equations for wave-averaged flow properites we start with the equations of motion and divide the basic flow properties u, v and d into long-period motions and the short-period wave contributions:

$$u = \langle u \rangle + \tilde{u}\,, \quad v = \langle v \rangle + \tilde{v}\,, \quad d = \langle d \rangle + \tilde{d}\,, \quad \langle \tilde{u} \rangle = \langle \tilde{v} \rangle = \langle \tilde{d} \rangle = 0. \tag{7.1}$$

Contributions to $\langle u \rangle$, $\langle v \rangle$ and $\langle d \rangle$ come from all motions whose typical time scale is significantly longer than the typical short-wave period. These can be for example either bound long waves associated with the set-down occurring under a group of short-period waves (Longuet-Higgins & Stewart 1964) or free long waves caused by a time-varying breakpoint (Symonds, Huntley & Bowen 1982) or any sort of current. On the other hand pure short-period contributions appear as correlations of wave-type terms (e.g. $\langle \tilde{u}\tilde{d} \rangle$, $\langle \tilde{u}\tilde{v} \rangle$, etc.).

By substituting in the shallow water equations (4.1) in this way for each flow variable and by phase averaging we obtain a set of equations for the long-period flow properties $\langle u \rangle$, $\langle v \rangle$ and $\langle d \rangle$:

$$\frac{\partial \langle d \rangle}{\partial t} + \frac{\partial}{\partial x}\left[\langle u \rangle \langle d \rangle + \langle \tilde{Q}_1 \rangle\right] + \frac{\partial}{\partial y}\left[\langle v \rangle \langle d \rangle + \langle \tilde{Q}_2 \rangle\right] = 0, \tag{7.2a}$$

$$\frac{\partial}{\partial t}\left[\langle u \rangle \langle d \rangle + \langle \tilde{Q}_1 \rangle\right] + \frac{\partial}{\partial x}\left[\langle d \rangle \left(\langle u \rangle^2 + \langle \tilde{u}^2 \rangle + \tfrac{1}{2}\langle d \rangle\right) + 2\langle u \rangle \langle \tilde{Q}_1 \rangle + \langle \tilde{S}_{11} \rangle\right]$$
$$+ \frac{\partial}{\partial y}\left[\langle d \rangle \left(\langle u \rangle \langle v \rangle + \langle \tilde{u}\tilde{v} \rangle\right) + \langle u \rangle \langle \tilde{Q}_2 \rangle + \langle v \rangle \langle \tilde{Q}_1 \rangle + \langle \tilde{S}_{12} \rangle\right] + \langle d \rangle = 0, \tag{7.2b}$$

$$\frac{\partial}{\partial t}\left[\langle v \rangle \langle d \rangle + \langle \tilde{Q}_2 \rangle\right] + \frac{\partial}{\partial y}\left[\langle d \rangle \left(\langle v \rangle^2 + \langle \tilde{v}^2 \rangle + \tfrac{1}{2}\langle d \rangle\right) + 2\langle v \rangle \langle \tilde{Q}_2 \rangle + \langle \tilde{S}_{22} \rangle\right]$$
$$+ \frac{\partial}{\partial x}\left[\langle d \rangle \left(\langle u \rangle \langle v \rangle + \langle \tilde{u}\tilde{v} \rangle\right) + \langle v \rangle \langle \tilde{Q}_1 \rangle + \langle u \rangle \langle \tilde{Q}_2 \rangle + \langle \tilde{S}_{12} \rangle\right] = 0, \tag{7.2c}$$

where $\langle \tilde{Q}_\mu \rangle = \langle \tilde{u}_\mu \tilde{d} \rangle$ is the mass flow due to wave motion while the contribution of the momentum flux due to wave motion is given by the the radiation stress term $\langle \tilde{S}_{\mu\nu} \rangle$.

This set of equations is not 'closed' unless a particular wave theory for the short-period wave field is adopted to compute terms like the mass flow and the radiation stress. For instance, it is common practice to use linear wave theory while dissipation effects induced by wave breaking are parameterized in the solution.

The breaking process is usually described in terms of simple properties and easy to compute parameters (Arcilla & Lemos 1990). For example a wave-breaking parameter such as the parameter B (see (3.13)) is adopted to prescribe initiation of breaking while another parameter D is introduced in order to model the wave energy dissipation and the related wave amplitude (height) decay. Many different models for the computation of the D-parameter are available; see for example Battjes & Janssen (1978) and Thornton & Guza (1983). A full review on this subject can be found in Battjes (1988).

Linear wave theory is not a good representation for the wave field near the shore. The Carrier & Greenspan (1958) solutions and their extension described above can be more appropriate. However, these solutions highlight an important property of the swash zone: incident waves may be reflected, partially reflected or fully absorbed. The Carrier & Greenspan solution corresponds to perfect reflection. In most studies with wave breaking the short waves are assumed to be fully absorbed, with any reflection being in the form of long, low-frequency waves.

To help crystallize ideas we note that one approach to this problem would be to extend the Carrier & Greenspan solution to $A\omega^3 > 1$ by computing the surf and swash zone behaviour for waves which have incoming Riemann invariants as for the Carrier & Greenspan solution with $A\omega^3 > 1$. The reflection, mass flow, radiation stress and the averaged swash zone properties, V, P and E could be tabulated as functions of A and ω. We assume that if a suitable model is found for the short-wave motion this can be described in terms of only an amplitude A and a frequency ω once the mean depth and mean flow velocity are given.

The types of equations that arise are perhaps seen most clearly in Hayes' (1973) extension of Whitham's approach. For sufficiently shallow water, the set of equations for unidirectional propagation is hyperbolic, and includes equations corresponding to (7.2*a*,*b*) for the mean flow, and two further equations for the wave propagation. Two characteristics of this set are the familiar pair for the shallow water equations; the other two, for the short waves, correspond to a splitting of the usual linear ray equation. That is, finite-amplitude effects split the rays into two characteristics, see Peregrine (1983) for another example of this. Both of these short-wave characteristics have velocities corresponding to a generalized group velocity plus the effects of varying depth and current due to larger scale motions. In the subsequent discussion we assume these to be known incident quantities in $x < x_l$.

Before discussing boundary conditions at the lower boundary of the swash zone, $x = x_l(y,t)$ we present a simpler example of a moving boundary, that is a rigid wall moving at velocity $U(t)\boldsymbol{i}$ which varies on a sufficiently slow time scale that its acceleration is unimportant.

The long-period motion has the known incoming Riemann variable

$$\alpha = 2\langle c \rangle + \langle u \rangle \tag{7.3}$$

and for an impermeable boundary the boundary condition is $\langle u \rangle = U(t)$. Thus the outgoing Riemann variable becomes

$$\beta = 2\langle c \rangle - \langle u \rangle = \alpha - 2U. \tag{7.4}$$

The incoming waves of amplitude A_{in}, wavenumber $\boldsymbol{k}_{in}$ and frequency ω_{in} are perfectly reflected at the wall, but to determine the outgoing values of A, $\boldsymbol{k}$ and ω the local behaviour at the moving wall must be considered.

In a frame of reference moving with the wall, the waves have an unchanging intrinsic frequency σ which is readily found from the Doppler shift:

$$\omega_{in} = \sigma + U\boldsymbol{i} \cdot \boldsymbol{k}_{in}. \tag{7.5}$$

The waves are perfectly reflected so that the outward propagating wave has $A_{out} = A_{in}$ and $\boldsymbol{k}_{out} = -(\boldsymbol{k}_{in} \cdot \boldsymbol{i})\boldsymbol{i} + (\boldsymbol{k}_{in} \cdot \boldsymbol{j})\boldsymbol{j}$ giving

$$\omega_{out} = \sigma + U\boldsymbol{i} \cdot \boldsymbol{k}_{out} = \sigma - U\boldsymbol{i} \cdot \boldsymbol{k}_{in} = \omega_{in} - 2U\boldsymbol{i} \cdot \boldsymbol{k}_{in}. \tag{7.6}$$

In comparing the moving swash zone boundary with the above simple boundary, we note:

(i) sufficient information must be available to determine the motion of the swash zone boundary, $x_l(t)$, as well as to determine β;

(ii) as above, a local wave model is needed to determine the properties of the outgoing wave, if any.

We concentrate on the first of these, and look at integration of swash zone equations similar to (4.2), or (4.3), to provide the necessary information. The integrated systems (4.2) and (4.3) are implicitly expressed in terms of the short-wave motions. There is now an important choice to be made: how much of the swash motion, if any, should be assigned to the long time scales? Consideration of the moving rigid wall example leads us to consider all motion relative to the point $x = x_l(y,t)$ to be short-wave motion and $x_l(y,t)$ to be 'driven' by the long-period motions. As a result, we consider all the quantities defined in tables 2 and 3 to be defined with velocities relative to x_l and also to be considered as known once incident short-wave parameters A_{in}, $\boldsymbol{k}_{in}$ and σ are known. That is quantities such as the mean volume of water in the swash zone, $\langle V \rangle$, are supposed to be known once the incoming short waves at $x = x_l$ are known.

Inside the swash zone most of the short-wave quantities, such as V, P_1, are also averaged over the short-wave motion and denoted by $\langle V \rangle$, $\langle P \rangle$ etc. and are to be determined from a short-wave model of the swash. There are exceptions for the longshore current quantities P_2, $M_{\mu 2}$ which are not entirely dependent on the local waves. When a bore, or flow which was near a bore, enters the swash zone it makes a large contribution to the longshore velocity, which often may only respond to bed friction on the longer time scale, e.g. see Ryrie (1983). This means that a decomposition of long-wave and short-wave contributions is also necessary within the swash zone.

We achieve this decomposition by assuming that swash motion is almost entirely assigned to short-wave contributions and that the only long-wave contribution comes from parameterizing the longshore drift due to wave breaking by a longshore current velocity $W = W(y,t)$. In similar fashion to equation (7.1), which applies outside the swash zone, we separate short-wave from long-wave contribution for the flow properties inside the swash zone:

$$d = \hat{d}\,, \quad u = \frac{\partial x_l}{\partial t} + \hat{u}\,, \quad v = W + \hat{v}\,, \tag{7.7a–c}$$

where a short-wave property inside the swash zone is defined as $\hat{G}$ rather than $\tilde{G}$ which pertains to short-wave contributions outside the swash zone. This decomposition permits the integrated terms depending on the longshore velocity to be divided

between long and short waves:

$$\langle P_2\rangle = \langle W\hat{V}\rangle + \langle \hat{P}_2\rangle\,, \tag{7.8a}$$

$$\langle M_{12}\rangle = \langle W\hat{P}_1\rangle + \langle \hat{M}_{12}\rangle + \frac{\partial x_l}{\partial t}\left(\langle W\hat{V}\rangle + \langle \hat{P}_2\rangle\right)\,, \tag{7.8b}$$

$$\langle M_{22}\rangle = \langle W^2\hat{V}\rangle + 2\langle W\hat{P}_2\rangle + \langle \hat{M}_{22}\rangle. \tag{7.8c}$$

All the integral properties which are to be considered as short-wave terms have a hat symbol. Using a different basis for short-wave and averaged quantities in the swash zone compared with those outside the swash zone may at first seem wayward. However, the character of swash motion is different: on many sandy beaches there is also a strong difference in the character of the bed in the swash zone compared with the bed just outside the swash zone.

In order to avoid greater complexity, the longshore variation of x_l has been assumed to be negligible in the above derivation. This is essentially a geometrical matter, and the above boundary conditions can be interpretated as being applicable when the x-direction is normal to the mean lowest boundary of the swash.

To obtain explicit expression of the first boundary condition we consider the flow of mass into the swash zone relative to $x = x_l$. The average of equation (4.2*a*) is

$$\frac{\partial\langle V\rangle}{\partial t} + \frac{\partial\langle P_2\rangle}{\partial y} = \langle Q_1\rangle|_{x_l} \tag{7.9}$$

where now the right-hand side contains the relative flow velocity $(u - \partial x_l/\partial t)$. The left-hand side is also rewritten in terms of the local variables inside the swash zone. After using (7.8*a*) for $\langle P_2\rangle$, integration across the swash zone width and averaging over the short waves we obtain

$$\frac{\partial\langle\hat{V}\rangle}{\partial t} + \frac{\partial\langle W\hat{V}\rangle}{\partial y} + \frac{\partial\langle\hat{P}_2\rangle}{\partial y} = \left\langle\left(u - \frac{\partial x_l}{\partial t}\right)d\right\rangle = \langle u\rangle\langle d\rangle + \langle\tilde{u}\tilde{d}\rangle - \frac{\partial x_l}{\partial t}\langle d\rangle\,. \tag{7.10}$$

The first term on the left-hand side of this equation is the rate of change of the total volume of water in the swash zone; the second and third terms are the change in volume due to the lateral variation of longshore currents respectively associated with the longshore velocity inside the swash zone W and with the wave contribution $\langle\hat{P}_2\rangle$. The right-hand side of (7.10) is the increase of water in the swash zone through its lower boundary; it is evaluated at $x = x_l$ using outer variables.

A similar derivation for the average balance of onshore momentum in the swash zone gives

$$\begin{aligned}
&\frac{\partial}{\partial t}\left[\langle\hat{P}_1\rangle + \frac{\partial x_l}{\partial t}\langle\hat{V}\rangle\right] + \frac{\partial\langle W\hat{P}_1\rangle}{\partial y} + \frac{\partial\langle\hat{M}_{12}\rangle}{\partial y}\\
&\quad + \frac{\partial x_l}{\partial t}\left[\frac{\partial\langle W\hat{V}\rangle}{\partial y} + \frac{\partial\langle\hat{P}_2\rangle}{\partial y}\right] + g\alpha\langle\hat{V}\rangle + \langle\Upsilon_1\rangle = \left\langle\left(u - \frac{\partial x_l}{\partial t}\right)^2 d + \tfrac{1}{2}gd^2\right\rangle\\
&\quad = \left(\langle u\rangle - \frac{\partial x_l}{\partial t}\right)^2\langle d\rangle + \tfrac{1}{2}g\langle d\rangle^2 + 2\langle\tilde{u}\tilde{d}\rangle\left(\langle u\rangle - \frac{\partial x_l}{\partial t}\right) + \langle\tilde{u}^2\rangle\langle d\rangle + \langle\tilde{u}^2\tilde{d}\rangle + \tfrac{1}{2}g\langle\tilde{d}^2\rangle.
\end{aligned} \tag{7.11}$$

In this equation dimensional expressions have been inserted to clarify the origin of terms. The first two terms on the left-hand side are the rate of change of the mean momentum in the swash zone. The group of terms with y-derivatives are the contribution from longshore velocity gradients which include both long-period

contributions (terms with W) and short-period contributions (terms with $\langle\hat{P}_2\rangle$ and $\langle\hat{M}_{12}\rangle$). The following terms are the action of gravity and friction on the water in the swash zone. The right-hand side is the momentum transfer into the swash zone at $x = x_l$ where the mean flow velocity relative to the swash zone limit appears in both long- and short-period terms. Finally pure short-period contributions appear. Conservation of longshore momentum similarly yields

$$\frac{\partial\langle W\hat{V}\rangle}{\partial t} + \frac{\partial\langle\hat{P}_2\rangle}{\partial t} + \frac{\partial\langle W^2\hat{V}\rangle}{\partial y} + 2\frac{\partial\langle W\hat{P}_2\rangle}{\partial y} + \frac{\partial\langle\hat{M}_{22}\rangle}{\partial y} + \langle Y_2\rangle$$
$$= \left\langle \left(u - \frac{\partial x_l}{\partial t}\right) vd \right\rangle$$
$$= \left(\langle u\rangle - \frac{\partial x_l}{\partial t}\right)\langle v\rangle\langle d\rangle + \langle\tilde{u}\tilde{v}\rangle\langle d\rangle + \langle\tilde{u}\tilde{d}\rangle\langle v\rangle + \langle\tilde{v}\tilde{d}\rangle\left(\langle u\rangle - \frac{\partial x_l}{\partial t}\right) + \langle\tilde{u}\tilde{v}\tilde{d}\rangle. \quad (7.12)$$

The above three equations are boundary conditions for the long-wave motion and x_l if the short-wave properties on each side of $x = x_l$ have 'known' models. Whereas in the rigid wall model only the boundary condition $\langle u\rangle = U(t)$ is required, now we also need to evaluate the changes in x_l and W. In addition, the short-wave models may be chosen to permit the reflection of short waves. Note, the short-wave swash model must be used relative to $x = x_l$, hence the motion of x_l is seen as the long-period contribution to the swash zone.

A delicate matter concerning the different wave models needed on each side of x_l also needs attention. There is no reason to suppose that W and $\langle v\rangle$ evaluated at $x = x_l$ should be equal; in fact they can be expected to differ since W describes a mean velocity of the swash zone. Thus when the average volume of water in the swash zone is diminishing, the right-hand side of equation (7.12) corresponds to longshore momentum leaving the swash zone and it seems to us that the terms with $\langle v\rangle$ would be better if $\langle v\rangle$ were replaced with W when $\mathrm{d}\langle\hat{V}\rangle/\mathrm{d}t$ is negative. We consider that this aspect of the boundary conditions needs further consideration which is best carried out in conjunction with further studies using particular models of the short-wave motions.

8. The short-wave contribution

In this section we briefly analyse the relevance of the short-wave contributions with particular emphasis on those appearing in the equations (7.10), (7.11) and (7.12) which are used to define the boundary conditions at the lower limit of the swash zone. Computation of the contributions has been performed by integrating the analytical solution for $A\omega^3 \leqslant 1$ and by integrating the fully numerical solution when wave breaking occurs, i.e. for $A\omega^3 > 1$.

Figure 17 shows the variation with the wave amplitude of the most relevant short-wave contributions when no wave breaking occurs, i.e. for $A\omega^3 < 1$. Those terms which are not shown since they are smaller than 10^{-6} are $\langle\hat{u}\hat{d}\rangle$, $\langle\hat{v}\hat{d}\rangle$, $\langle\hat{u}\hat{v}\rangle$, $\langle\hat{u}\hat{v}\hat{d}\rangle$, $\langle\hat{P}_1\rangle$ and $\langle\hat{M}_{12}\rangle$. The largest term is $\langle\hat{u}^2\rangle$ while $\langle\hat{d}^2\rangle$ and $\langle\hat{u}^2\hat{d}\rangle$ are one order of magnitude smaller. The three integral flow properties shown in figure 17 are monotonic increasing functions of the wave amplitude. Note that curves in figures 17 to 19 have been obtained by joining discrete points which represent the results of single computations. This explains the lack of smoothness in some of the curves.

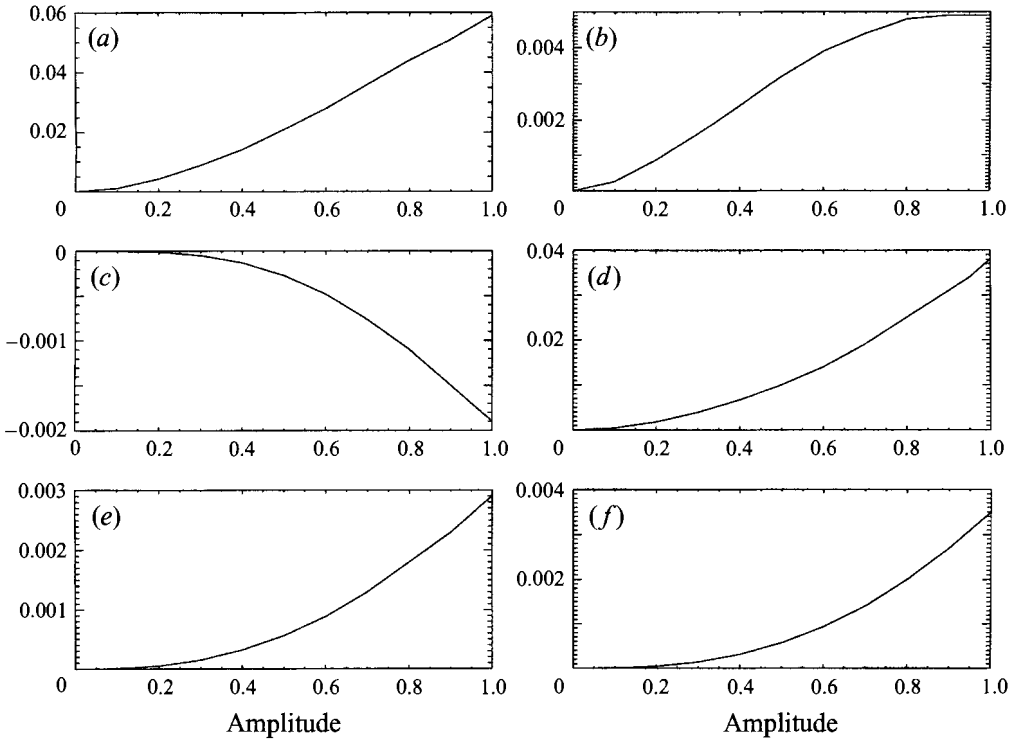

FIGURE 17. Short-wave contribution at the boundary x_l and inside the swash zone for wave frequency $\omega = 1$ and for no-wave-breaking conditions. From top left to bottom right they are the short-wave averages (*a*) $\langle \hat{u}^2 \rangle$, (*b*) $\langle \hat{d}^2 \rangle$, (*c*) $\langle \hat{u}^2 \hat{d} \rangle$ and the integral properties (*d*) $\langle \hat{V} \rangle$, (*e*) $\langle \hat{P}_2 \rangle$, (*f*) $\langle \hat{M}_{22} \rangle$.

For waves that break, momentum and energy are transferred from the short waves to the longshore currents; different terms need to be taken into account as major contributions to equations (7.10), (7.11) and (7.12), see figure 19. A first evident difference between the non-breaking and the breaking case is related to the swash zone width $x_h - x_l$. The non-breaking solution predicts a linearly monotonic increasing swash zone width with respect to both wave amplitude and wave frequency (see (3.3)):

$$x_h - x_l = \tfrac{1}{2} A\omega. \tag{8.1}$$

On the other hand for periodic wave-breaking solutions there appears to be an asymptotic size for the swash zone width, see figure 18. This may account for the reduced rate of increase in mean volume $\langle \hat{V} \rangle$ inside the swash zone with respect to that typical of the non-breaking waves (see figures 17*d* and 19(*c*)). We have yet to investigate the interesting maximum of $\langle \hat{u}^2 \rangle$ near $A\omega^3 = 3$.

A more substantial difference arises in the longshore motion, for which the approximate equation (2.7*c*) is used to give a solution for the averaging. The input of longshore momentum from the bores is balanced by bed friction but generally on the longer time scale. Although bores die out when they meet the shoreline and cause run-up, the water that forms the swash has acquired longshore momentum from the bore before it enters the swash zone. A fully detailed consideration of this case also awaits further study; here we present the rate of change in time of the quantities $\langle P_2 \rangle$, $\langle M_{12} \rangle$ and $\langle M_{22} \rangle$.

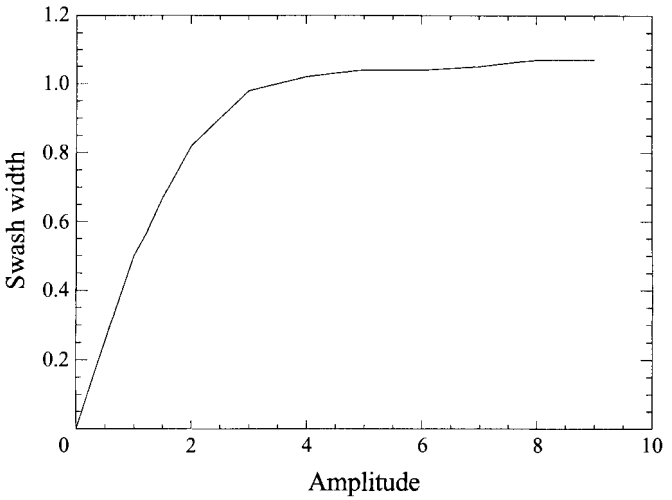

FIGURE 18. Swash zone width as function of the wave amplitude. Carrier & Greenspan solution ($\omega = 1$), as extended numerically for $A > 1$.

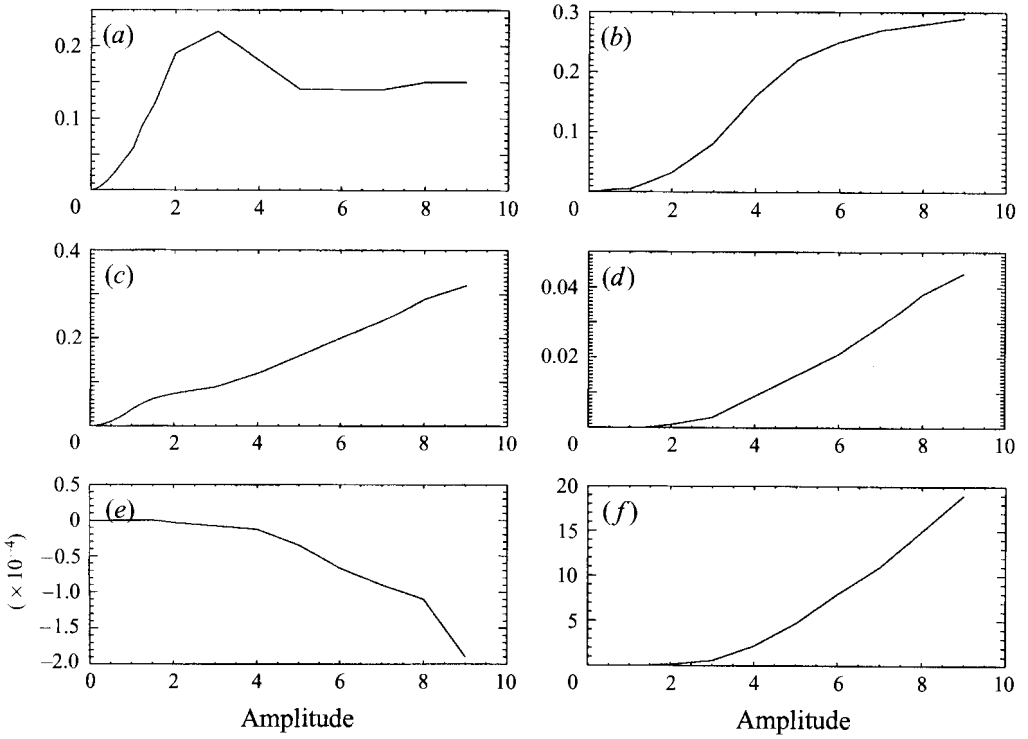

FIGURE 19. Short-wave contribution at the boundary x_l and inside the swash zone for wave frequency $\omega = 1$. From top left to bottom right they are the short-wave correlations (*a*) $\langle \hat{u}^2 \rangle$, (*b*) $\langle \hat{a}^2 \rangle$ the integral properties (*c*) $\langle \hat{V} \rangle$, and the rate of change of the three global integral properties (*d*) $\langle P_2 \rangle$, (*e*) $\langle M_{12} \rangle$ and (*f*) $\langle M_{22} \rangle$. Note that for $A \leqslant 1$ numerical integration of the analytical solution is shown while for $A > 1$ fully numerical solution of the NLSWE is represented.

The figures presented here indicate that not all the terms that are introduced into the boundary conditions (7.10), (7.11) and (7.12) are necessary. Further investigation should help to clarify both which are the most significant terms when considered in the context of the equations and what are the effects of friction terms.

9. Conclusions

This paper is an initial study of flow properties in the swash zone using the nonlinear shallow water equations, it ranges from explicit detailed solutions to averaged equations.

A weakly three-dimensional extension of the two-dimensional solution by Carrier & Greenspan (1958) of the nonlinear shallow water equations for waves sloshing on an inclined plane beach is developed and used to illustrate the further ideas. The solution represents standing wave modes generated by perfect reflection at the shore of the incoming waves. However this particular solution can only be used until breaking conditions, i.e. a vertical wave front, are reached. For larger values of the wave amplitude solutions with bores are modelled by numerically solving the nonlinear shallow water equations.

There is not a unique definition of the mean shoreline. On the contrary some different definitions are analysed and discussed with explicit computation for each definition based on the analytic Carrier & Greenspan (1958) solution, e.g. the mean water depth is different at each position.

Flow properties in the swash zone are similar to those in the region between trough and crest for freely propagating surface waves. In particular the Stokes' drift of water waves has its counterpart in the swash zone as a longshore drift. Such a flow associated with the swash zone is essentially a mass flux, which in averaging needs to be associated with the chosen shoreline position or boundary for the swash zone. In fact we have found it most convenient to take the lower boundary of the swash zone as the line that bounds the sea. By integrating across the swash zone a simplified swash zone model is found. It shows promise for use in wave-resolving numerical models, since it captures most of swash zone features and if required can give a reasonable spatial model of the flow.

A study of averaging of the swash zone to provide boundary conditions for wave-averaged models is given. It is intended to lay the foundations for further, more practical development, by indicating the basic equations obtained from such averaging. Instead of the single boundary condition needed at a simple boundary two further conditions are found in order to determine the motion of swash zone boundary and the mean longshore flow in the swash zone. The short-wave motions are assumed to come from 'known' models. The determination of suitable short-wave models for surf and swash zones is a subject for further study, but an indication of the way forward is given by evaluating swash zone properties for the extended Carrier & Greenspan solution and its numerical extension to include bores.

This work was supported by the European Community, Directorate Generale XII under the two contracts: Human Capital and Mobility ERBCHBICT930678 and MAS2-CT92-0047. We wish to thank Dr Gary Watson for many useful conversations, and the referees for their contribution to improving the clarity of our presentation.

REFERENCES

ARCILLA, S. A. & LEMOS, C. M. 1990 *Surf Zone Hydrodynamics.* Centro Internacional de Metodos Numericos en Ingeniera, Barcelona.

BATTJES, J. A. 1988 Surf-zone dynamics. *Ann. Rev. Fluid. Mech.* **20**, 257–293.

BATTJES, J. A. & JANSSEN, J. P. F. M. 1978 Energy loss and set-up due to breaking in random waves. *Proc. 16th Intl Conf. on Coastal Engineering, ASCE*, pp. 569–587.

CARRIER, G. F. 1966 Gravity waves on water of variable depth. *J. Fluid Mech.* **24**, 641–659.

CARRIER, G. F. 1971 Dynamics of tsunamis. In *Mathematical Problems in the Geophysical Sciences. Vol. 1: Geophysical Fluid Dynamics* (ed. W. H. Reid). American Mathematical Society.

CARRIER, G. F. & GREENSPAN, H. P. 1958 Water waves of finite amplitude on a sloping beach. *J. Fluid Mech.* **4**, 97–109.

DODD, N. 1994 On the destabilization of a longshore current on a plane beach: Bottom shear stress, critical conditions, and onset of instability. *J. Geophys. Res.* **99**, 811–824.

GALVIN, C. J. 1972 Wave breaking in shallow water. In *Waves on Beaches and Resulting Sediment Transport* (ed. R. E. Meyer). Academic Press.

HANSON, B. A. 1926 The theory of ship waves. *Proc. R. Soc. Lond.* A **111**, 491–529.

HASSELMANN, K. 1971 On the mass and momentum transfer between short gravity waves and larger-scale motions. *J. Fluid Mech.* **50**, 189–205.

HAYES, W. D. 1973 Group velocity and nonlinear dispersive wave propagation. *Proc. R. Soc. Lond.* A **332**, 199–221.

HIBBERD, S. & PEREGRINE, D. H. 1979 Surf and run-up on a beach: a uniform bore. *J. Fluid Mech.* **95**, 323–345.

HO, D. V. & MEYER, R. H. 1962 Climb of a bore on a beach. Part 1. Uniform beach slope. *J. Fluid Mech.* **14**, 305–318.

KELLER, J. B. 1963 Tsunamis - Water waves produced by earthquakes. In *Proc. Tsunami Meetings Associated with the Tenth Pacific Science Congress, 1991. IUGG Monograph*, Vol. 24 (ed. D. C. Cox). Published for the Institut Geographique National, Paris.

KOBAYASHI, N., OTTA, A. K. & ROY, I. 1987 Wave reflection and run-up on rough slopes. *Proc. ASCE* **113** (WW3), 282–298.

LONGUET-HIGGINS, M. S. & STEWART, R. W. 1964 Radiation stresses in water waves: a physical discussion, with applications. *Deep-Sea Res.* **11**, 529–562.

MEI, C. C. 1983 *The Applied Dynamics of Ocean Surface Waves.* John Wiley and Sons. (Current edition: World Scientific.)

MEYER, R. E. & TAYLOR, A. D. 1972 Run-up on beaches. In *Waves on Beaches and Resulting Sediment Transport* (ed. R. E. Meyer). Academic Press.

NIELSEN, P. 1989 Wave setup and runup: an integrated approach. *Coast. Engng.* **13**, 1–9.

PACKWOOD, A. R. 1980 Surf and run-up on a beach. PhD thesis, University of Bristol.

PEREGRINE, D. H. 1972 Equations for water waves and the approximations behind them. In *Waves on Beaches and Resulting Sediment Transport* (ed. R. E. Meyer). Academic Press, New York.

PEREGRINE, D. H. 1983 Wave jumps and caustics in the propagation of finite-amplitude water waves. *J. Fluid Mech.* **136**, 435–452.

RYRIE, S. C. 1983 Longshore motion generated on beaches by obliquely incident bores. *J. Fluid Mech.* **129**, 193–212.

SHEN, M. C. & MEYER, R. E. 1963 Climb of a bore on a beach. Part 3. Run-up. *J. Fluid Mech.* **16**, 113–125.

STOKER, J. J. 1947 *Water Waves.* Interscience.

STOKES, G. G. 1847 On the theory of oscillatory waves. *Trans. Camb. Phil. Soc.* **8**, 441–455.

SVENDSEN, I. A. & LORENZ, R. S. 1988 Velocities in combined undertow and longshore currents. *Coast Engng* **13**, 55–79.

SVENDSEN, I. A. & PUTREVU, U. 1994 Nearshore mixing and dispersion. *Proc. R. Soc. Lond.* A **445**, 561–576.

SYMONDS, G., HUNTLEY, D. A. & BOWEN, A. 1982 Two-dimensional surf beat: long wave generation by a time-varying break-point. *J. Geophys. Res.* **87**, 492–498.

SYNOLAKIS, C. E. 1987 The run-up of solitary waves. *J. Fluid Mech.* **185**, 523–545.

THORNTON, E. B. & ABDELRAHMAN, S. 1991 Sediment transport in the swash due to obliquely incident wind-waves modulated by infragravity waves. *Proc. Coastal Sed. '91*, pp. 100–113.

THORNTON, E. B. & GUZA, R. T. 1983 Transformation of wave height distribution. *J. Geophys. Res.* **88**, 5925–5938.

VAN DONGEREN, A. R., SANCHO, F. E., SVENDSEN, I. A. & PUTREVU, U. 1994 SHORECIRC: a quasi 3-D nearshore model. *Proc. 24th Intl Conf. on Coastal Engineering, Kobe, ASCE*, vol. 3, pp. 2741–2754.

WATSON, G., BARNES, T. C. D. & PEREGRINE, D. H. 1994 The generation of low frequency waves by a single wave group incident on a beach. *Proc. 24th Intl Conf. on Coastal Engineering, Kobe, ASCE*, vol. 1, pp. 776–790.

WATSON, G., PEREGRINE, D. H. & TORO, E. F. 1992 Numerical solution of the shallow-water equations on a beach using the weighted average flux method. In *Computational Fluid Dynamics '92 - Vol. 1* (ed. Ch. Hirsh *et al.*), pp. 495–502. Elsevier.

WHITHAM, G. B. 1979 *Lectures on Wave Propagation.* Published for the Tata, Institute of Fundamental Research, Bombay by Springer.